

1 **Comparing temperature data sources for use in species distribution models:**  
2 **from *in-situ* logging to remote sensing**

3 ***Running header: temperature data for distribution models***

4 Jonas J. Lembrechts<sup>1,\*</sup>, Jonathan Lenoir<sup>2</sup>, Nina Roth<sup>3</sup>, Tarek Hattab<sup>4,2</sup>, Ann Milbau<sup>5</sup>, Sylvia  
5 Haider<sup>6,7</sup>, Loïc Pellissier<sup>8,9</sup>, Aníbal Pauchard<sup>10,11</sup>, Amanda Ratier Backes<sup>6,7</sup>, Romina D.  
6 Dimarco<sup>12</sup>, Martin A. Nuñez<sup>13</sup>, Juha Aalto<sup>14,15</sup>, Ivan Nijs<sup>1</sup>

7 <sup>1</sup> *Centre of Excellence Plants and Ecosystems (PLECO), University of Antwerp, 2610 Wilrijk,*  
8 *Belgium*

9 <sup>2</sup> *UR “Ecologie et Dynamique des Systèmes Anthropisés” (EDYSAN, UMR 7058 CNRS-*  
10 *UPJV), Université de Picardie Jules Verne, 1 Rue des Louvels, 80037 Amiens Cedex 1,*  
11 *France*

12 <sup>3</sup> *Biogeography and Geomatics, Department of Physical Geography, Stockholm University,*  
13 *10691 Stockholm, Sweden*

14 <sup>4</sup> *MARBEC (IRD, Ifremer, Université de Montpellier, CNRS), Sète Cedex, France*

15 <sup>5</sup> *Research Institute for Nature and Forest - INBO, Havenlaan 88, bus 73, 1000 Brussels,*  
16 *Belgium*

17 <sup>6</sup> *Institute of Biology / Geobotany and Botanical Garden, Martin Luther University Halle-*  
18 *Wittenberg, Halle (Saale), Germany*

19 <sup>7</sup> *German Centre for Integrative Biodiversity Research (iDiv) Halle-Jena-Leipzig, Leipzig,*  
20 *Germany*

21 <sup>8</sup> *Landscape Ecology, Institute of Terrestrial Ecosystems, ETH Zürich, CH-8092 Zürich,*  
22 *Switzerland*

23 <sup>9</sup> *Swiss Federal Research Institute WSL, CH-8903 Birmensdorf, Switzerland*

24 <sup>10</sup> *Laboratorio de Invasiones Biológicas, Facultad de Ciencias Forestales, Universidad de*  
25 *Concepción, Casilla 160-C, 4030000 Concepción, Chile*

26 <sup>11</sup> *Institute of Ecology and Biodiversity (IEB), 8320000 Santiago, Chile*

27 <sup>12</sup> *Grupo de Ecología de Poblaciones de Insectos, INTA-CONICET, Modesta Victoria 4450,*  
28 *8400, Bariloche, Argentina*

29 <sup>13</sup> *Grupo de Ecología de Invasiones, INIBIOMA, CONICET-Universidad Nacional del*  
30 *Comahue, Av. de Los Pioneros 2350, 8400 Bariloche, Argentina*

31 <sup>14</sup> *Dept of Geosciences and Geography, Gustaf Hällströmin katu 2a, FIN-00014 Univ. of*  
32 *Helsinki, Finland*

33 <sup>15</sup> *Finnish Meteorological Inst., Finland*

34 *\*Corresponding author: [jonas.lembrechts@uantwerpen.be](mailto:jonas.lembrechts@uantwerpen.be), +3232651727.*

35 *Orcid ID JJL: [orcid.org/0000-0002-1933-0750](https://orcid.org/0000-0002-1933-0750).*

36 *Orcid ID JL: [orcid.org/0000-0003-0638-9582](https://orcid.org/0000-0003-0638-9582).*

37 *Orcid ID TH: [orcid.org/0000-0002-1420-5758](https://orcid.org/0000-0002-1420-5758).*

38 *Orcid ID AM: [orcid.org/0000-0003-3555-8883](https://orcid.org/0000-0003-3555-8883).*

39 *Orcid ID SH: [orcid.org/0000-0002-2966-0534](https://orcid.org/0000-0002-2966-0534).*

40 *Orcid ID AP: [orcid.org/0000-0003-1284-3163](https://orcid.org/0000-0003-1284-3163).*

41 *Orcid ID JA: [orcid.org/0000-0001-6819-4911](https://orcid.org/0000-0001-6819-4911)*

42

43

#### 44 **Acknowledgements**

45 The research leading to this publication has received funding from the Research Foundation-

46 Flanders (FWO) through a personal grant to JJL, from the European INTERACT-program

47 through a Transnational Access grant to JJL and through the Methusalem funding of the

48 Flemish Community through the Research Council of the University of Antwerp.

49 Computational resources and services were provided where needed by the HPC core facility

50 CalcUA of the University of Antwerp, and VSC (Flemish Supercomputer Center), funded by

51 the Research Foundation - Flanders (FWO) and the Flemish Government – department EWI.

52 AP funded by CONICYT PFB-23 and Fondecyt 1180205. The authors declare no conflicts of

53 interest.

#### 54 **Biosketch**

55 This study is performed in the framework of (1) the Mountain Invasion Research Network

56 (MIREN, [www.mountaininvasions.org](http://www.mountaininvasions.org)), a global consortium of plant ecologists focussing on

57 species redistributions in mountain regions, and (2) SoilTemp (<https://soiltemp.weebly.com>),

58 a global effort to create a database of in-situ soil temperature measurements for use in

59 ecology.

60

61

62

63

64 **Abstract**

65 **Aim:** While species distribution models (SDMs) traditionally link species occurrences to free-  
66 air temperature data at coarse spatiotemporal resolution, the distribution of organisms might  
67 rather be driven by temperatures more proximal to their habitats. Several solutions are  
68 currently available, such as downscaled or interpolated coarse-grained free-air temperatures,  
69 satellite-measured land surface temperatures (LST) or *in-situ* measured soil temperatures. A  
70 comprehensive comparison of temperature data sources and their performance in SDMs is  
71 however currently lacking.

72 **Location:** Northern Scandinavia

73 **Time period:** 1970 - 2017

74 **Major taxa studied:** Higher plants

75 **Methods:** We evaluated different sources of temperature data (WorldClim, CHELSA,  
76 MODIS, E-OBS, topoclimate and soil temperature from miniature data loggers), differing in  
77 spatial resolution (1'' to 0.1°), measurement focus (free-air, ground-surface or soil  
78 temperature) and temporal extent (year-long vs. long-term averages), and use them to fit  
79 SDMs for 50 plant species with different growth forms in a high-latitude mountain region.

80 **Results:** Differences between these temperature data sources originating from measurement  
81 focus and temporal extent overshadow the effects of temporal climatic differences and  
82 spatiotemporal resolution, with elevational lapse rates ranging from -0.6 °C per 100 m for  
83 long-term free-air temperature data to -0.2 °C per 100 m for in-situ soil temperatures. Most  
84 importantly, we found that the performance of the temperature data in SDMs depended on  
85 species' growth forms. The use of in-situ soil temperatures improved the explanatory power

86 of our SDMS ( $R^2$  on average +16%), especially for forbs and graminoids ( $R^2$ : +24% and  
87 +21% on average, respectively) compared to the other data sources.

88 **Main conclusions:** We suggest future studies using SDMs to use the temperature dataset that  
89 best reflects the species' ecology, rather than automatically using coarse-grained data from  
90 WorldClim or CHELSA.

91

92 **Keywords:** bioclimatic variables, climate change, growth forms, microclimate, mountains,  
93 land surface temperature, bioclimatic envelope modelling, soil temperature, species  
94 distribution modelling

## 95 **Introduction**

96 Species distribution models (SDMs) are widely used to describe and forecast the spatial  
97 distribution of species (Elith & Leathwick, 2009). SDMs relate species occurrence data with  
98 information about the environmental conditions at these locations (Guisan & Thuiller, 2007;  
99 Elith & Leathwick, 2009; Jiménez-Valverde *et al.*, 2011). The most common strategy is to  
100 work with long-term (e.g. 30 years) interpolated averages of a set of bioclimatic variables at  
101 30'' resolution (ca. 1 × 1 km at the equator), e.g. WorldClim or CHELSA (Hijmans *et al.*,  
102 2005; Warren *et al.*, 2008; Sears *et al.*, 2011; Slavich *et al.*, 2014; Gonzalez-Moreno *et al.*,  
103 2015; Karger *et al.*, 2017). While such macroclimate data might be sufficient to capture the  
104 conditions on flat terrains, many environments host a heterogeneous topography (e.g. across  
105 steep elevational gradients in mountain regions) that make the microclimate near the ground  
106 vary noticeably over short distances (Gottfried *et al.*, 1999; Holden *et al.*, 2011; Scherrer &  
107 Körner, 2011; Sears *et al.*, 2011; Opedal *et al.*, 2015; Stewart *et al.*, 2018). In order to make  
108 realistic forecasts of species distributions and distribution shifts in such heterogeneous  
109 environments, it has been suggested that climate data at finer spatiotemporal resolutions are  
110 needed (Illan *et al.*, 2010; Scherrer & Körner, 2011; Graae *et al.*, 2012; Lenoir *et al.*, 2013;  
111 Opedal *et al.*, 2015; Graae *et al.*, 2018). Such new climate datasets including *in-situ* logging  
112 and remote sensing are now increasingly becoming available (Bramer *et al.*, 2018). Yet, an  
113 evaluation of their performance in species distribution models is necessary to provide  
114 guidance for future studies, in particular those predicting species responses to climate change  
115 (Stewart *et al.*, 2018).

116 In the high-latitude and high-elevation areas of northern Europe, local temperatures have been  
117 found to vary up to 6° C within 1 km<sup>2</sup> spatial units, reflecting the local topography (Lenoir *et*  
118 *al.*, 2013). This high temperature variation depends for instance on the interaction between  
119 temperature and snow distribution, and consequently affects the length of the local growing

120 season (Körner, 2003; Aalto *et al.*, 2018). Local temperatures also vary strongly between  
121 seasons, and short-term extreme weather conditions have been shown to be more relevant for  
122 species distributions than the average climatic conditions (Ashcroft & Gollan, 2012).  
123 Including this variation into SDMs is likely to be crucial, for instance in the context of  
124 stepping stones, holdouts or microrefugia (Dobrowski, 2011; Opedal *et al.*, 2015; Meineri &  
125 Hylander, 2017). Stepping stones refer to areas with microclimates that facilitate species'  
126 range shifts, e.g. upward or poleward movement during climate change or after non-native  
127 species introductions (Pauchard *et al.*, 2009; Hannah *et al.*, 2014; Lembrechts *et al.*, 2017).  
128 Holdouts and microrefugia on the other hand are areas with a relatively stable microclimate  
129 where isolated populations can persist for a certain time (Ashcroft, 2010; Hannah *et al.*, 2014;  
130 Lenoir *et al.*, 2017; Meineri & Hylander, 2017). Climatic variability within an area can indeed  
131 considerably buffer climate warming effects (Lenoir *et al.*, 2013; Lenoir *et al.*, 2017), which  
132 often remains undetected using macroclimate data, possibly leading to the overestimation of  
133 rates of extinction and range expansion (Willis & Bhagwat, 2009).

134 Moreover, many organisms (particularly small-stature plants, certain types of insects and soil  
135 microbes) experience temperatures at ground or sub-surface level, which can differ strongly  
136 from ambient air temperatures that are usually measured at 2 m above the soil surface (Poorter  
137 *et al.*, 2016; Aalto *et al.*, 2018; Körner & Hiltbrunner, 2018). Especially in high-latitude and  
138 high-elevation regions, snow cover for example acts as an insulator, thereby strongly  
139 decoupling soil and air temperatures (Pauli *et al.*, 2013; Poorter *et al.*, 2016; Thompson *et al.*,  
140 2018), while biophysical processes due to vegetation cover may also decouple upper  
141 atmospheric conditions from boundary layer conditions (Geiger, 1950).

142 In order to overcome this spatiotemporal mismatch between climate data and species ecology  
143 and to improve predictions of species' current and future distributions, four main approaches  
144 are commonly used: (i) to downscale existing coarse-grained (i.e. 1000 x 1000 m resolution)

145 climate data (McCullough *et al.*, 2016); (ii) to interpolate climate station data (Aalto *et al.*,  
146 2017), (iii) to gather local climate data through field measurements (Potter *et al.*, 2013;  
147 Slavich *et al.*, 2014; Lenoir *et al.*, 2017); or (iv) to monitor climatic conditions continuously  
148 in space and time through remote sensing technologies (e.g. satellite-measured land surface  
149 temperatures) (Wan, 2008; Metz *et al.*, 2014; Neteler *et al.*, 2014). In the first two approaches,  
150 a high spatial resolution can be obtained using topographic variables derived from digital  
151 elevation models which are available at much finer resolutions (e.g. 1'', which is about 30 ×  
152 30 m at the equator). Such downscaled or interpolated climate data has been found to be a  
153 significant improvement over macroclimatic variables for modelling species distributions  
154 (Randin *et al.*, 2009b; Dobrowski, 2011; Slavich *et al.*, 2014; Meineri & Hylander, 2017).

155 In the third approach, one uses actual *in-situ* measurements to provide fine-grained climatic  
156 conditions with high spatial accuracy (microclimate) (Opedal *et al.*, 2015; Meineri &  
157 Hylander, 2017). Such field measurements can also be interpolated to the level of regional  
158 climate using topographical information (Ashcroft *et al.*, 2008; Maclean *et al.*, 2017; Greiser  
159 *et al.*, 2018), yet usually cover short temporal and small geographical extents only. In addition  
160 to a fine spatial resolution, *in-situ* measurements provide the opportunity to adapt the  
161 measurement focus to the ecology or life form of the species, e.g. by measuring near-surface  
162 soil temperature instead of air temperature. Gathering *in-situ* temperature data, however,  
163 requires considerably more resources than the previously mentioned downscaling approaches  
164 (Opedal *et al.*, 2015; Meineri & Hylander, 2017). Increasing the spatiotemporal resolution and  
165 extent of such field measurements generally refines the predictions, but also presents a  
166 logistical challenge (Wundram *et al.*, 2010; Meineri & Hylander, 2017).

167 Finally, the fourth approach, i.e. using remotely sensed data, is now more frequently used in  
168 SDMs (Pottier *et al.*, 2014), for instance through remotely sensed snow cover data or by using  
169 the normalized difference vegetation index (NDVI) (Yannic *et al.*, 2014). One such remotely

170 sensed source of data of which the spatiotemporal resolution, extent and accuracy is rapidly  
171 improving is satellite-based land-surface temperatures (LST) (Wan, 2008; Wan *et al.*, 2015).  
172 Remotely-sensed LST are now freely available at the global scale at the vegetation canopy or  
173 land surface level, with a temporal resolution of days over a period of decades and with a  
174 spatial resolution ranging from 30'' (ca. 1000 × 1000 m at the equator) to as fine as 1'' (ca. 30  
175 × 30 m) (Cook, 2014). This type of data does have the advantage over free-air temperature  
176 datasets like WorldClim or CHELSA of being a direct and contiguous measurement in space  
177 and time, as opposed to data interpolation and temporal averaging from a network of weather  
178 stations, yet might be strongly affected by land surface characteristics and cloud cover in the  
179 area (Zellweger *et al.*, 2019). Thanks to the increasing availability of these long-term and  
180 accurate time series, such satellite-based LST-datasets offer very promising research avenues  
181 to fill the gap between local temperature measurements and global-scale climatic datasets.

182 These different approaches to obtain suitable climate data have been extensively explored  
183 and applied in SDMs (Bramer *et al.*, 2018), yet a comparative study of all of these  
184 (downscaled and interpolated macroclimate data, field measurements, and satellite-based  
185 LST) together – both concerning their inherent characteristics and their role in SDMs - has up  
186 till now been missing. Such a comparison is nevertheless urgently needed in order to quantify  
187 the progress that can be made by replacing the traditional global climate models with other  
188 temperature data sources. We hypothesize in that regard that the best result depends in large  
189 on two critical factors: a) the climatic characteristics of the study region, and b), the growth  
190 forms of the study organisms. Here, we use a case study along steep climatic gradients in the  
191 Northern Scandes, a mountain range in northern Scandinavia, to assess both factors and to  
192 provide guidelines for the use of temperature data in SDMs in topographically challenging  
193 regions. We compare the characteristics of different temperature datasets within the region, as  
194 well as the descriptive and predictive power of SDMs for 50 plant species with different



195 growth forms: forbs, graminoids, (dwarf) shrubs and trees. We compare global climate  
196 datasets (i.e. WorldClim and CHELSA) with datasets of remotely-sensed LST (MODIS), a  
197 topographic downscaling and interpolation approach, and soil temperature obtained with  
198 miniature data loggers, and use three widely applied and ecologically relevant (i.e.  
199 bioclimatic) temperature variables: (i) mean annual temperature and mean temperature of the  
200 (ii) warmest and (iii) coldest quarter. We hypothesize a significant effect of the spatial  
201 resolution of the climate data, as well as of measurement focus (free-air, surface, or soil) and  
202 temporal extent on temperature patterns across topographic gradients. Increasing  
203 spatiotemporal accuracy of temperature data, especially through the use of *in-situ*  
204 measurements, is expected to improve the descriptive and predictive power of the SDMs,  
205 despite the associated loss in temporal extent. The optimal resolution, extent and  
206 measurement focus are, however, likely to depend on the growth forms of the assessed  
207 species, i.e. the spatiotemporal framework in which they operate.

## 208 **Methods**

### 209 ***Study region***

210 The study was conducted in the Northern Scandes mountain range in Norway and Sweden,  
211 between N 67°46'23.5" / E 16°30'52.6" (south west) and N 68°40'33.6" / E 18°58'40.4"  
212 (north east), covering an area of 100 × 100 km and an elevation range from 0 up to 2097 m  
213 a.s.l. The area ranges from the Norwegian coast, with a relatively mild and wet climate  
214 dominated by birch forests with heathland understory, to the significantly drier and colder  
215 eastern side of the Northern Scandes, typically vegetated by subarctic, alpine dwarf shrub  
216 vegetation (Lembrechts *et al.*, 2014). The region was chosen for its strong climatic gradient,  
217 with large macro- and microclimatic variation due to a distinct topography and high latitude

218 location (Scherrer & Körner, 2011; Graae *et al.*, 2012; Lenoir *et al.*, 2013). In total, 106  
219 temperature measurement locations were spread across the study area (Fig. 1).

## 220 *Climate data*

221 For this area, we obtained eight different types of climate data encompassing a wide range of  
222 measurement foci, spatiotemporal resolutions and temporal extents (Table 1). For each of  
223 these datasets, we extracted or calculated the mean annual temperature and mean temperature  
224 of the warmest and coldest quarter (bioclimatic variables Bio1, Bio10 and Bio11, following  
225 the definition of WorldClim, Hijmans *et al.*, 2005, hereafter called mean annual, summer and  
226 winter temperature, respectively). These ecologically relevant variables belong to the set of  
227 physiologically most pertinent bioclimatic determinants of spatial plant species distribution  
228 and are thus commonly used in SDMs (e.g. Austin & Van Niel, 2011; Cord & Rödder, 2011;  
229 Distler *et al.*, 2015), and they allow us to accurately take into account seasonal differences in  
230 climate. The different datasets are discussed in detail below.

### 231 a) WorldClim

232 The WorldClim database (Version 2.0) provides globally interpolated free-air temperature  
233 conditions over a 30-year time period (1970-2000) at a spatial resolution of 30'' (ca. 1000 ×  
234 1000 m at the equator) (Fick & Hijmans, 2017). The studied bioclimatic variables were  
235 directly downloaded from the website ([www.worldclim.org](http://www.worldclim.org)).

### 236 b) CHELSA

237 The climatologies at high resolution for the earth's land surface areas (CHELSA, Version 1.2)  
238 is a global dataset based on quasi-mechanistical statistical downscaling of free-air  
239 temperatures from the ERA Interim (ECMWF) global circulation model (Dee *et al.*, 2011),  
240 over a period of 34 years (1979-2013) and with the same spatial resolution as WorldClim

241 (30'', ca. 1000 x 1000 m at the equator), yet for a more recent time period (Karger *et al.*,  
242 2017). Bioclimatic variables were again downloaded directly from the website ([www.chelsa-](http://www.chelsa-climate.org)  
243 [climate.org](http://www.chelsa-climate.org)).

244 c) Downscaled CHELSA-data (hereafter called 'downscaled')

245 We used the bioclimatic variables downloaded from CHELSA, at an original resolution of  
246 30'' (ca. 1000 x 1000 m at the equator), and downscaled them statistically even further, to a  
247 1'' (ca. 30 x 30 m at the equator) resolution based on topographic variation, using a  
248 physiographically-informed model fitted with a geographically weighted regression (GWR)  
249 technique (Fotheringham *et al.*, 2003). In short, GWR extends the traditional regression  
250 approach by allowing estimated regression parameters to vary across space. Therefore, GWR  
251 models are particularly relevant to explore the scale-dependent and spatial non-stationary  
252 relationships between free-air temperatures and physiographic variables (here: elevation,  
253 slope, eastness, northness, distance to the ocean and clear-sky solar radiation) (Su *et al.*,  
254 2012). For more details, see Supplementary Material 1.

255 d) Topoclimate

256 Fine-resolution gridded climate data for the region was obtained from Aalto *et al.* (2017), who  
257 included topography-driven small-scale climate heterogeneity in a topoclimatic interpolation  
258 of weather station data across northern Scandinavia, using generalized additive modelling at a  
259 resolution of 1'' (ca. 30 x 30 m at the equator). They modelled monthly average temperatures  
260 from 1981 till 2010 using geographical location, elevation, water cover, solar radiation and  
261 cold-air pooling. Bioclimatic variables were calculated based on these monthly averages.

262 e) MODIS LST

263 The moderate resolution imaging spectroradiometer (MODIS) satellite TERRA (Wan *et al.*,  
264 2015) from the National Aeronautics and Space Administration (USA) provides global land  
265 surface temperature (LST). We extracted data from MOD11A2: 8-day averages based on the  
266 clear sky day- and night-time records at a 30'' (ca. 1000 × 1000 m at the equator) resolution,  
267 for a period of two years corresponding to the *in-situ* measurements (from August 2015 to  
268 July 2017, see below). Mean annual temperature was calculated in ArcGIS by averaging the  
269 temperature per pixel for 2015-2016 and 2016-2017, separately, from day of the year (DOY)  
270 209 in year *n* (e.g. July 27th for 2015) till DOY 208 in year *n*+1 (e.g. July 26th for 2016),  
271 which was the set of 8-day averages corresponding most closely with the period used for the  
272 *in-situ* temperature measurements described below (see sub-section *h* on Soil temperatures).  
273 Mean summer and winter temperatures were calculated similarly, yet for DOY 185 (e.g. July  
274 3th in 2015) till 272 (September 28th in 2015) and from DOY 1 (e.g. January 1st in 2016) till  
275 88 (March 28th in 2016), respectively.

276 f) EuroLST

277 The EuroLST dataset is a gap-filled dataset at the European scale of LST derived from  
278 MODIS (see sub-section *e* focusing on MODIS LST) at a spatial resolution of 250 × 250 m  
279 and averaged over a temporal extent of 10 years (Metz *et al.*, 2014). This dataset has been  
280 created using a combination of weighted temporal averaging with statistical modelling and  
281 spatial interpolation to fill in the gaps in the MODIS LST dataset, as well as to improve its  
282 spatial resolution. Relevant bioclimatic variables were downloaded directly from the website  
283 ([courses.neteler.org/eurolst-seamless-gap-free-daily-european-maps-land-surface-](https://courses.neteler.org/eurolst-seamless-gap-free-daily-european-maps-land-surface-temperatures)  
284 [temperatures](https://courses.neteler.org/eurolst-seamless-gap-free-daily-european-maps-land-surface-temperatures)).

285 g) E-OBS

286 The E-OBS dataset (version 17.0) provides daily gridded climate data of free-air temperature  
287 for Europe at a  $0.1^\circ$  (ca.  $10.000 \times 10.000$  m at the equator) spatial resolution, interpolated  
288 from weather stations (Haylock *et al.*, 2008), used here over the study period from August  
289 2015 to July 2017 (as in sub-section *e* on MODIS LST). The gridded dataset is created by first  
290 interpolating the monthly mean temperature from the weather stations using three-  
291 dimensional thin-plate splines, interpolating the daily anomalies using a spatial kriging  
292 approach with an external drift for temperature, and then combining these monthly and daily  
293 estimates. Temperature data was downloaded directly from the website  
294 (<https://www.ecad.eu/download/ensembles/download.php>) and subsequently used to generate  
295 the three studied bioclimatic variables in R.

#### 296 h) Soil temperatures

297 Near-surface soil temperatures were logged every 1.5 or 2 hours (iButtons: DS1922L or  
298 DS1921G, with  $0.5^\circ\text{C}$  accuracy, [www.maximintegrated.com](http://www.maximintegrated.com), San José, CA, USA) at a depth  
299 of 3 cm below the soil surface in 106 locations along several elevation gradients in Norway  
300 and Sweden (Fig. 1, Table 2). Loggers were wrapped in parafilm and put in a small zipper bag  
301 to prevent water damage. The loggers were originally established for several different projects  
302 (Lembrechts *et al.*, 2014; Lembrechts *et al.*, 2016; Lembrechts *et al.*, 2017) along seven  
303 elevation gradients, together ranging from 0 to 1200 m a.s.l., of which three were in Norway  
304 and four in Sweden. The three bioclimatic variables were calculated in R (R Core Team,  
305 2015) for each 106 locations and for each year (from 2015 till 2017, corresponding to the  
306 periods used in sub-section *e*) from daily averages. Based on these soil temperature data, we  
307 made predictions for each bioclimatic variable for the whole study area of  $100 \times 100$  km for  
308 the period August 2016 till July 2017 using GWRs (as in sub-section *c* featuring the  
309 downscaling approach) based on the same physiographic variables (i.e. elevation, slope,  
310 eastness, northness, distance to the ocean and clear-sky solar radiation). The models were

311 used to predict the bioclimatic variables for every 1'' (ca. 30 x 30 m at the equator) pixel in  
312 the study area. For more details on the interpolation approach, see Supplementary Material 1.

### 313 ***Plant species observations***

314 Plant species data were obtained during summer 2017 in the framework of the Mountain  
315 Invasion Research Network ([www.mountaininvasions.org](http://www.mountaininvasions.org)) long-term monitoring effort, and  
316 specifically as a follow-up of the survey of Lembrechts *et al.* (2014) in the Norwegian study  
317 plots (59 out of the 106 plots with *in-situ* soil temperature measurements, see Fig. 1, Table 2).  
318 Within the framework of this survey, three elevation gradients were selected (spanning on  
319 average 700 m in elevation). The elevation range covered by each gradient was divided into  
320 19 equally spaced elevation bands, resulting in 20 sampling sites per gradient. At each  
321 elevation, presence/absence of all vascular plant species was recorded in plots of 2 x 50 m in  
322 natural vegetation. At one end of each of these plots, the temperature logger (see dataset  
323 described in sub-section *h* above) was buried. We used data for the 50 most common plant  
324 species in the survey (i.e. at least 10 occurrences). Species were grouped based on their  
325 growth forms (Table S1): forbs (N = 25); graminoids (N = 7); dwarf shrubs (N = 15); and  
326 trees (N = 3). All species were native to the region.

### 327 ***Direct comparison of climatic variables***

#### 328 1) Relation to elevation

329 To assess differences in the behaviour of the eight climate datasets along an elevation  
330 gradient, the three bioclimatic variables derived from these climate datasets were plotted  
331 separately against the elevation of the 106 locations of the *in-situ* soil temperature data  
332 loggers. For the gridded climate datasets, we extracted a value for each bioclimatic variable  
333 for each location. We used linear models (function *lm* in R, R Core Team, 2015) to assess the  
334 lapse rate (i.e. the slope, °C per 100 m) of temperature decrease with elevation. For MODIS

335 LST, E-OBS and the soil temperature measurements, data was plotted and modelled  
336 separately for the two study years (2015-2016 and 2016-2017).

#### 337 2) Paired comparisons

338 For each of the 106 studied locations, we compared the values for each climatic dataset (and  
339 each of the three bioclimatic variables) against the others, to investigate consistent  
340 temperature deviations between datasets. Trends for each bioclimatic variable and each  
341 dataset were visualised with general additive models (GAMs) with a cubic regression line and  
342 without pre-set smoothing value (function `gam`, R package `mgcv`, Wood, 2006), following  
343 procedures described in Zuur *et al.* (2009). GAMs were used as we did not want to make  
344 restrictive assumptions about the relationships of the datasets with each other.

#### 345 3) Correlative dendrograms

346 For all 106 locations, we made correlative dendrograms (distance =  $1 - \rho$ , where  $\rho$  is the  
347 Pearson's product-moment correlation) to visualize correlations among and relationships  
348 between the different datasets, using the function `hclust` from the package `spatstat` (Baddeley  
349 *et al.*, 2015).

#### 350 4) Regional climate predictions

351 We generated regional maps for the different climate datasets (see the Climate data section as  
352 well as Supplementary Material 1 for more details on how the maps were generated for the in-  
353 situ measurements), and calculated for each pixel the absolute temperature difference between  
354 the respective dataset and the regionally modelled soil temperature at a 1'' (ca. 30 × 30 m at  
355 the equator) spatial resolution.

#### 356 5) Temporal correction

357 For a more formal comparison between the datasets with different temporal windows, we  
358 calculated for each climatic dataset its difference with the ‘background climate’, taken as  
359 temperatures for the window in question from the ERA Interim (ECMWF) 2 meter free-air  
360 temperature database (Dee *et al.*, 2011). This is a time series of monthly means of daily means  
361 from 1979 up till 2018 (hence covering the time period for all studied datasets except  
362 WorldClim), for which we calculated average Bio1, Bio10 and Bio11 over the whole 100 ×  
363 100 km study area (based on the original 0.75° × 0.75° resolution grid). We then re-ran the  
364 paired comparisons (see above) with the temperature off-set, i.e. the difference between the  
365 bioclimatic value (for each observation and for each dataset) and the average bioclimatic  
366 value from ERA Interim for the corresponding period, using paired t-tests to test for potential  
367 differences, e.g. differences between a) Bio1(soil temperature<sub>(2016-2017)</sub>) – Bio1(ERA  
368 Interim<sub>(2016-2017)</sub>) and b) Bio1(CHELSA<sub>(1979-2013)</sub>) – Bio1(ERA Interim<sub>(1979-2013)</sub>).

369 Using this off-set of temperatures from a standardized and common time series allowed to  
370 correct to some extent for differences in the temporal scope among the climatic datasets, and  
371 thus climate change and inter-annual weather variation. While this does not take into account  
372 possible decoupling of climate change between soil, surface and air temperature, it does allow  
373 to estimate the size of the temporal effect in the dataset, and thus quantify the difference  
374 between in-situ soil temperature and the other datasets more precisely.

### 375 ***Species distribution modelling***

376 The regional distribution of the 50 plant species was modelled using species-specific  
377 generalized linear mixed-effect models (GLMMs) (function *glmer*, package *lme4* (Bates *et*  
378 *al.*, 2013), family = binomial) as a function of mean annual, summer and winter temperature,  
379 and their quadratic terms. Gradient (plant data were available from three different elevation  
380 gradients; Table 2) was used as a random intercept term in these models to account for



381 structural variation between gradients. This was repeated for each climate dataset (except for  
382 E-OBS, as due to the limited measured climate variation within the region, species  
383 distributions could not be modelled), resulting in a total of 350 SDMs (50 species  $\times$  7  
384 datasets). For both MODIS LST and soil temperature, only the data from the measurement  
385 year prior to the species observations (2016-2017) were used, while the bioclimatic variables  
386 from 2015-2016 were highly correlated with those of 2016-2017 and thus excluded. The  
387 variance inflation factor (VIF, function `vif`, package `car`, Fox & Weisberg, 2011) was  
388 calculated for each of the climatic datasets to test the correlation between the different  
389 bioclimatic variables. As the VIF (a value between 0 and infinity) exceeded 5 (indicating a  
390 strong correlation) for some datasets (specifically those with long-term climatic averages),  
391 separate models including only Bio1 as explanatory variables were made, and results  
392 compared between both approaches.

393 The explained variance in the present distribution of the species ( $R^2$  of the fixed effect, i.e. the  
394 marginal  $R^2$ , Nakagawa & Schielzeth, 2013) was then calculated for each model and  
395 compared across all species between the different datasets with an ANOVA and a post-hoc  
396 Tukey HSD test ( $R^2 \sim$  growth forms (factor with 4 levels), model assumptions were met). We  
397 also compared the increase in  $R^2$  values obtained by using soil temperature versus the other  
398 climate datasets for the different growth forms (forbs, graminoids, shrubs and trees)  
399 separately.

400 Finally, we assessed the predictive power of the different SDMs using a leave-one-out  
401 method, each time calibrating the model with 59 data points (plots) and predicting for the  
402 remaining one. We calculated the area under the curve (AUC) of the receiver operation  
403 characteristic (ROC), using the function `performance` from the package `ROCR` (Sing *et al.*,  
404 2005), as well as the sensitivity (presences correctly predicted as presences) and the  
405 specificity (absences correctly predicted as absences) metrics. A value of 0.5 was used to

406 binarize predictions. This was repeated for each species and for each climate dataset, and  
407 differences in AUC, sensitivity and specificity between SDMs using the different climatic  
408 datasets were again assessed with an ANOVA and a post-hoc Tukey HSD test. We also  
409 compared the increase in AUC, sensitivity and specificity obtained by using soil temperature  
410 versus the other climate datasets for the different growth forms separately. Note that this  
411 predictive approach is limited for three reasons: First, the restricted dataset size likely  
412 constrains the predictive power of the models. Secondly, for comparison purposes, our SDMs  
413 are only calibrated using bioclimatic predictors, and thus predictive power (as estimated here  
414 using AUC-values) will be relatively low. Thirdly, when using predictive modelling in small-  
415 sized plots (i.e. 100 m<sup>2</sup> here, vs. 1 km<sup>2</sup> traditionally), one can expect a high accuracy in  
416 correctly predicting presences as presence (i.e. if a species is observed, the model will also  
417 predict its presence), yet low accuracy in predicting absences as absence (i.e. if a species is  
418 absent, this could either be due to the plot falling outside its niche (correctly predicted  
419 absence), or due to random absences due to the limited plot size, or microscale non-climatic  
420 factors (incorrectly predicted absence)). Of course, incorrect absences can also be due to  
421 observation bias, identification uncertainties and incomplete detection, further lowering  
422 predictive power. We thus expect high sensitivity, yet relatively low specificity and AUC-  
423 values, and encourage interpretation of these different evaluation metrics together to assess  
424 the predictive power of the models (Jiménez-Valverde, 2012).

425 All analyses were performed in R (R Core Team, 2015).

## 426 **Results**

### 427 *Direct comparison of climatic variables*

428 All three studied bioclimatic variables (Bio1 = mean annual, Bio10 = mean summer and  
429 Bio11 = mean winter temperature) showed a consistent negative correlation with elevation in

430 almost all temperature datasets in the region, yet with large differences in lapse rate (Fig. 2).  
431 The latter ranged for mean annual temperature from around  $-0.6$  °C per 100 m for CHELSA,  
432 downscaled CHELSA and Topoclimate, over around  $-0.4$  °C per 100 m for WorldClim,  
433 EuroLST and MODIS LST to  $-0.2$  °C per 100 m for soil temperature and  $-0.1$  °C per 100 m  
434 for E-OBS. Mean annual temperatures were in both years consistently higher for the soil  
435 temperature than for all other datasets, i.e. both the long-term temperature data (WorldClim,  
436 CHELSA, downscaled CHELSA, Topoclimate and EuroLST, Fig. 3a-e) and the surface  
437 (MODIS LST, Fig. 3f) and free-air (E-OBS, Fig. 3g) temperature measurements from the  
438 same time period ( $p < 0.001$  from a linear model), yet differences were larger at low than at  
439 high temperatures. Differences of 3 to 6 °C between soil temperature and all other datasets  
440 remained even after correcting for possible inter-annual and climate change effects (Table 3,  
441 Fig. S1a-f). Significant differences of up to 3 °C in mean annual temperature could also be  
442 observed between all other datasets (Table 4, Fig. S2).

443 Despite the higher mean annual temperature in the soil, mean summer soil temperature was in  
444 both years similar (compared to WorldClim, Topoclimate, EuroLST and E-OBS) or even  
445 lower (CHELSA, downscaled CHELSA and MODIS LST) than air and surface temperature  
446 (Fig. 3h-n). After correcting for inter-annual and climate change effects, differences between  
447 soil temperature and most other datasets (except MODIS LST) remained limited to around 1  
448 to 1.5 °C (Table 4, Fig. S1g-l). Summer temperature recordings were highest in MODIS LST  
449 (Fig. 2n, Fig. S2i,k,l). The relationship with elevation was again the strongest for  
450 (downscaled) CHELSA ( $-0.6$  °C per 100 m), and weakest for E-OBS and MODIS LST.

451 Winter temperature showed the largest discrepancy between soil, free-air and surface  
452 temperatures (Fig. 3), with soil temperatures being close to 0 °C from sea level up to at least  
453 900 m a.s.l., and as such driving the higher mean annual temperatures in the soil (Fig. 2x).  
454 Part of this variation was due having relatively warm winters with plenty of snow in the area

455 in the period 2015-2017, yet the difference remained as high as 4 °C to 11 °C after correcting  
456 for the temporal mismatch (Table 4, Fig. S1n-r). Surface temperatures were in addition colder  
457 than free-air temperatures (Fig. S2n-r) due to an extended frost period (Fig. S3). Temperature  
458 differences between years were relatively small, except for mean annual and mean summer  
459 surface temperatures from MODIS (Fig. 2f,n).

460 The above-mentioned differences along the elevation gradient, combined with additional  
461 effects from local topography, resulted in large regional differences between the different  
462 climate datasets in general (Fig. 4), and between interpolated soil temperature and the other  
463 datasets in particular (Fig. 5). The correlation analyses (Fig. 4) showed that the climate  
464 datasets were nested, with strongest relationships (across all bioclimatic variables) between  
465 the datasets with long-term averages: (downscaled) CHELSA, Topoclimate, WorldClim and  
466 EuroLST. The datasets with short-term measurements (in-situ soil, MODIS LST and free-air  
467 E-OBS) differed more from each other than from the long-term averages. Modelled mean  
468 annual temperature in the soil was, as expected, several degrees warmer than in all other  
469 datasets, especially at higher elevations (Fig. 5), while in summer soil temperature was  
470 warmer than CHELSA climate and MODIS LST at high elevations, yet colder at low  
471 elevations (Fig. 5). Winter temperature predictions were up to 17 °C higher in the soil than in  
472 the other datasets, except at the highest elevations. Due to the large local variation in snow  
473 cover, however, winter soil temperature predictions were unreliable (Fig. 5, Fig. S3), in  
474 contrast to annual and summer temperatures, for which the local  $R^2$  (indicating the local  
475 spatial regression fit) of the regional interpolations was highly consistent across space, albeit  
476 only moderately high, i.e. on average 50% for Bio10 and 37% for Bio1.

#### 477 *Species distribution modelling*

478 SDMs using soil temperatures explained on average 80% of variance (48% if only Bio1 was  
479 used), which was on average 18% (15% for models with Bio1 only) more than the models  
480 using other climate datasets (Fig. 6, significant differences with most datasets after correcting  
481 for multiple testing). Differences in explained variance among SDMs based on these other  
482 datasets were much smaller. Differences in predictive power were not significant between  
483 models (highest for Euro-LST and downscaled CHELSA (AUC  $\approx$  0.70), and between 0.61  
484 and 0.64 for the other datasets (Fig. S5). As expected, sensitivity was high ( $\approx$  0.85), yet  
485 specificity was low ( $\approx$  0.27) for all datasets. Predictive modelling was nearly impossible with  
486 models with Bio1 only (AUC  $\approx$  0.5, specificity  $\approx$  0.20), even though sensitivity was still high  
487 ( $\approx$  0.81).

488 Model performances depended strongly on growth forms (i.e. forbs, graminoids, dwarf  
489 shrubs, trees, Fig. 6b-c). We observed a significant net improvement in marginal  $R^2$  values (as  
490 an indicator of descriptive power of the models) for SDMs based on soil temperature in the  
491 case of forbs and graminoids compared to the other datasets (on average +24% and +21% for  
492 the full model, respectively, and 20% and 25% for the model with Bio1 only), and moderately  
493 so for shrubs (full model: +8%, Bio1: +25%). Yet there was no such net increase for trees  
494 (+2% and 8% only). On the contrary, we observed a significant net decrease in predictive  
495 values for shrubs and trees when using soil temperature compared to most of the other  
496 datasets (AUC on average -0.12 and -0.11 respectively for both models; -0.06 and -0.08 for  
497 Se), yet not so for forbs and graminoids (Fig. S5b-c).

## 498 **Discussion**

499 Our comparison of different climate datasets highlights that the use of a specific source of  
500 climate data is species- and region-specific and can have strong repercussions on the outcome  
501 of SDMs, as exemplified here for the distributions of 50 plant species along steep climatic

502 gradients in a cold-climate region. Our data indeed revealed a strong sensitivity of SDMs to  
503 the used climate dataset depending on the growth form of the species. In general, the use of  
504 *in-situ* soil temperature instead of surface or free-air temperature did improve the explanatory  
505 power of our SDMs. It did so much more for forbs and graminoids, to a lesser degree for  
506 shrubs, yet not for trees (Fig. 6). This outcome confirms recent studies arguing for the use of  
507 more local climate variables in distribution modelling (e.g. Ashcroft *et al.*, 2008; Pradervand  
508 *et al.*, 2014; Slavich *et al.*, 2014; Opedal *et al.*, 2015; Meineri & Hylander, 2017) and proofs  
509 the validity of this concept across a whole range of possible temperature data sources. Yet,  
510 our results also indicate that an increased accuracy of climate data does not necessarily  
511 improve distribution models for all species or in all circumstances (Bennie *et al.*, 2014;  
512 Pradervand *et al.*, 2014), as it will depend on the growth forms of the species and perhaps also  
513 the regional climate characteristics. The differences in SDMs' explanatory power could result  
514 from differences in measurement focus and spatiotemporal resolution or extent, related to the  
515 different spatiotemporal framework in which different species groups operate, as discussed  
516 below.

### 517 ***Measurement focus***

518 The most critical differences observed between the climate datasets in this study were likely  
519 driven by measurement focus (free-air, land surface or soil), with consistently higher average  
520 annual temperatures observed in the soil resulting to a large extent from differences in winter  
521 temperatures (Bio11). Even though free-air temperature predictions (WorldClim, CHELSA,  
522 E-OBS) for winter temperature easily dropped below -7 °C, and surface temperature  
523 measurements (EuroLST, MODIS LST) were even lower, winter temperatures just below the  
524 soil surface were close to 0 °C along most of the elevation gradient (Fig. 2). Only in those  
525 locations where global climate models predicted an average winter temperature below -10 °C,  
526 measured soil temperatures dropped below 0 °C (Fig. 2). These differences remained even

527 after correcting for the temporal mismatch in the different datasets (Table 4, Fig. S1). While  
528 some of the earliest studies on soil temperature reported a strong relationship with air  
529 temperature across all seasons (Shanks, 1956), it is clear that both a dense vegetation cover  
530 and a thick snowpack can provide effective insulation and protection against freezing events  
531 in the subnivium (Geiger, 1950; Dorrepaal *et al.*, 2004; Pauli *et al.*, 2013; Aalto *et al.*, 2017;  
532 Thompson *et al.*, 2018), and that snow in the Arctic is a crucial explanatory variable for the  
533 distribution of plant species (Randin *et al.*, 2009a; Niittynen & Luoto, 2017). In northern  
534 Norway, especially, the relatively mild climate and humid air from the ocean result in thick  
535 winter snow packs that can provide a significant decoupling between air, surface and soil  
536 temperature (Pauli *et al.*, 2013; Thompson *et al.*, 2018). Such an insulating snow pack can  
537 affect plant life in several ways, through its effects on overwintering survival, productivity,  
538 reproductive success and nutrient and water availability (Niittynen & Luoto, 2017), with both  
539 positive (e.g. less frost events) and negative effects (e.g. limited growing season) observed.  
540 For many species in the region, especially low-growing forbs and graminoids, we have shown  
541 that using near-surface soil temperatures instead of free-air temperatures, which allows  
542 incorporating these snow cover effects, is crucial to accurately describe the distribution of  
543 small-stature plants (Randin *et al.*, 2009a; Niittynen & Luoto, 2017). For trees, however, the  
544 absence of model improvement through the use of soil temperature might result from a  
545 stronger correlation with air than with soil temperature due to higher maximum canopy  
546 heights, at least in later life stages. In winter and early spring, trees are likely to be much more  
547 affected by air temperatures and freezing events affecting their buds above the snow than by  
548 temperatures in the soil (Körner, 2003).

549 These results also indicate that the relative importance of using soil temperature in SDMs will  
550 depend on the topography and large-scale climate of the region. Most importantly, the amount  
551 of fresh snow in winter will define the strength of the discrepancy between winter (and thus

552 indirectly annual) mean temperatures in the soil and in the air (Cohen, 1994; Zhang, 2005).  
553 The mismatch is in our study indeed significantly larger in the warmer but snowier  
554 (Norwegian) plots at low elevations than in the colder yet drier (Swedish) plots at high  
555 elevations (Fig. 3). For summer temperature, our data overall showed a more consistent  
556 match between the different datasets, although with minor buffering effects of the vegetation.  
557 Even though the discrepancy between measurement foci is thus region-specific (and likely  
558 even more different in e.g. tropical regions), we suggest that the use of climate data in close  
559 proximity to the study species is always recommended. Importantly, however, the use of soil  
560 temperature does not fully resolve this measurement mismatch, as only part of the plants are  
561 belowground. Although our data demonstrates a significant improvement in the use of soil  
562 temperature over free-air temperature data for species groups entirely covered by snow in  
563 winter, an optimal approach would incorporate in-situ climate measurements both above and  
564 below the soil surface. The latter can for example be achieved with the temperature and soil  
565 moisture plant simulator sensors as described in Wild *et al.* (2019), measuring temperatures  
566 at, above and below the surface.

567 Despite the clear benefits of using soil temperature data in SDMs, a major drawback (next to  
568 the cost associated with obtaining *in-situ* soil temperature measurements) lies in the increased  
569 local-scale heterogeneity, especially in winter. The soil temperatures were in our study indeed  
570 hard to predict accurately using a 50 × 50 m DEM-based interpolation approach. More *in-situ*  
571 temperature measurements, as well as the inclusion of other microclimate-related variables  
572 like snow cover maps, might be needed to improve interpolations of microclimate at fine  
573 spatial resolution. This is also a prerequisite for better SDMs' predictive performances.  
574 Follow-up studies with larger datasets and in-situ measurements of more environmental  
575 variables (e.g. soil moisture, air temperature, precipitation, or snow cover) are thus  
576 recommended to investigate this further.



577 While satellite-measured land surface temperature data (MODIS LST and EuroLST) resulted  
578 in mean annual temperatures within the same range as those obtained with free-air  
579 temperature measurements, the land surface temperatures were, throughout the measurement  
580 period, significantly higher in summer and lower in winter, thus resulting in an increased  
581 overall annual temperature range (Fig. 2, Fig. S1, Table 4). These extremes were however  
582 smoothed out when using the EuroLST temperature averages over a ten-year period. While  
583 the use of satellite-based land surface temperature for SDMs has until now been largely  
584 underexplored, our study adds to the growing list of recent studies indicating the potential of  
585 these untapped data resources for accurately predicting species distributions (see e.g. Cord &  
586 Rödder, 2011; Bisrat *et al.*, 2012; Neteler *et al.*, 2013). We expect that LST-timeseries with an  
587 even higher spatial resolution, such as Landsat (Cook, 2014) will as such turn out the crucial  
588 link between local-scale temperature measurements and global climate models. Our results  
589 however indicate that smoothed, long-term averages like EuroLST are preferable above short-  
590 term measurements, especially for predictive modelling. Similar to the issue of spatial  
591 heterogeneity for *in-situ* soil temperature data, averages over long-term time series are, by  
592 nature, more likely to increase the predictive performances of SDMs compared with more  
593 erratic fluctuations based on short-term data.

#### 594 ***Temporal - extent***

595 Differences between the used climate datasets could also be attributed to variation in temporal  
596 extent, with the datasets building on long-term historic averages (WorldClim, CHELSA,  
597 Topoclimate and EuroLST) showing the strongest correlation with each other (Fig. 4).  
598 Correlations were however weakest for the three datasets with only two years of data, yet with  
599 different measurement foci as described above (MODIS LST, E-OBS and soil temperature).  
600 While patterns over time for these datasets were relatively consistent between measurement  
601 years (Fig. 2), they did reveal more variation between air and surface temperature than

602 between EuroLST and the other datasets with long-term climatic averages. The discrepancy in  
603 temporal extents might also explain why the performance of our predictive models decreased  
604 in some cases for shrubs and trees when using short-term soil (or surface) temperatures (Fig.  
605 S4 and 5). These long-lived species are indeed likely to be relatively inert towards short-term  
606 changes in their environment (Körner, 2003), which might make it harder to predict their  
607 distribution based on locally-measured short-term temperatures (Ashcroft *et al.*, 2008). Long-  
608 lived organisms like most arctic-alpine species in the study region could also persist outside  
609 their niche for considerable parts of their life (Bond & Midgley, 2001), adding to the  
610 complexity of predicting their distribution using short-term temperature data.

### 611 ***Spatial resolution***

612 Our comparative approach indicates that the downscaling or interpolation of climate data – as  
613 applied here respectively to global datasets like CHELSA and the *in-situ* soil temperature  
614 data and topoclimatic dataset from Aalto *et al.* (2017) – was rather successful. Downscaling  
615 of CHELSA from 1000 × 1000 m to 30 × 30 m based on the physiography worked well, as  
616 indicated by the high local R<sup>2</sup>-values (0.90 ± 0.06 for Bio1 and Bio10, 0.89 ± 0.06 for Bio11,  
617 Fig. S4), yet nevertheless only resulted in minor improvements of the regional SDMs  
618 compared to coarse-grained CHELSA-data (3.7% and 0.035 for the R<sup>2</sup> and AUC values,  
619 respectively). This lack of improvement is in disagreement with several other studies (e.g.  
620 Gillingham *et al.*, 2012; Slavich *et al.*, 2014). Part of this could be due to the inherent  
621 limitations in the original CHELSA dataset: unlike elevation, small-scale topographic  
622 variables like slope and aspect are not taken into account into the original CHELSA model,  
623 and their inclusion in the downscaling approach is thus unlikely to have major effects. Small-  
624 scale topographic effects on microclimate are more correctly taken into account in the  
625 topoclimatic dataset from Aalto *et al.* (2017), however, making the latter approach  
626 recommendable above the former. The fact that the topoclimatic dataset did not perform

627 significantly better in the SDMs than CHELSA either ( $\Delta R^2 = -7\%$  and  $+5\%$ , and  $AUC = -0.01$   
628 and  $+0.06$ , depending on the model), might suggest again that an increased level of detail is  
629 not better by default, yet depends on the context of the study (Bennie *et al.*, 2014). The most  
630 likely explanation for this lack of improvement in model performance in this case thus is that  
631 the distribution of the studied alpine species might be less driven by small-scale topoclimatic  
632 variation in air temperature than by snow-cover induced variation in soil temperature.

633 Interpolation of the soil temperature data worked well across the whole study region, except  
634 for winter temperature, where probably the strong local variation and the highly non-linear  
635 correlation with elevation resulted in inaccurate predictions (Figure 4, Fig. S3, Ashcroft *et al.*,  
636 2008). The large differences in winter temperatures between measurement locations – and the  
637 low predictability of soil winter temperature in the region – thus suggest that caution is  
638 needed, as in many regions winter temperatures are likely crucial for the distribution of  
639 species (Williams *et al.*, 2015). A larger dataset and more accurate predictor variables, e.g.  
640 related to snow cover duration (Niittynen & Luoto, 2017), might be needed to improve these  
641 interpolation efforts.

## 642 ***Implications***

643 The observed differences in the climate datasets and SDMs at the regional scale advocate for  
644 a careful selection of the climate data source when modelling species distributions, based on a  
645 priori ecological assumptions about the relationship of the studied organism with the regional  
646 environment, and the comparison – or joint use – of different datasets (Buermann *et al.*, 2008;  
647 Rebaudo *et al.*, 2016). Measurement focus, temporal extent and spatiotemporal resolution  
648 should all be taken into account with regard to the studied species and area: is the species  
649 affected by snow cover; is it an annual or a perennial species; is the focal species mobile or  
650 sessile; does the study area reach above the treeline; is it in topographically challenging

651 terrain, etc. Our study highlights the importance of growth forms: soil temperature was highly  
652 important for forbs and graminoids, and to a certain extent for shrubs, yet not so for trees.  
653 Only when making ecologically meaningful a priori decisions, and when comparing the  
654 performance of different datasets – and perhaps their interactions, one can be sure that the  
655 observed trends relate to the actual (micro)climate experienced by the study species or species  
656 group(s) in the study region. Understanding these processes in the current climate is a crucial  
657 step before model projections can be improved under climate change as well. In order to  
658 advance towards this goal, there is an urgent need for large-scale datasets of microclimate  
659 data; ecologists and climatologists should consider in-depth on-the-ground, long-term  
660 microclimate monitoring along climatic gradients to be able to improve our microclimatic  
661 models for use in SDMs (Lembrechts *et al.*, 2018). Nevertheless, our case study suggests that  
662 SDMs can be relatively robust to several characteristics of different types of climate datasets,  
663 like spatial and temporal resolution, especially in the relatively stable slow-reacting  
664 vegetation types of high-latitude mountains. Additionally, there is a need to improve our  
665 abilities to forecast microclimate data itself in the future, as climate change is likely to affect  
666 soil, surface and air temperatures differently (Ashcroft & Gollan, 2013; De Frenne *et al.*,  
667 2019). Significant progress has been made in this regard, for example by integrating  
668 microclimatic dynamics and processes like microclimatic buffering in predictions (Keppel *et*  
669 *al.*, 2015; Lenoir *et al.*, 2017; Wason *et al.*, 2017), yet there is still a need for improvement  
670 before the same diversity and quality of climate datasets will be available for SDM  
671 projections into future climate as we have now for current climate.

## 672 **References**

673 Aalto, J., Riihimäki, H., Meineri, E., Hylander, K. & Luoto, M. (2017) Revealing topoclimatic  
674 heterogeneity using meteorological station data. *International Journal of Climatology*, **37**,  
675 544-556.

676 Aalto, J., Scherrer, D., Lenoir, J., Guisan, A. & Luoto, M. (2018) Biogeophysical controls on soil-  
677 atmosphere thermal differences: implications on warming Arctic ecosystems. *Environmental*  
678 *Research Letters*, **13**, 074003.

679 Ashcroft, M.B. (2010) Identifying refugia from climate change. *Journal of Biogeography*, **37**, 1407-  
680 1413.

681 Ashcroft, M.B. & Gollan, J.R. (2012) Fine-resolution (25 m) topoclimatic grids of near-surface (5 cm)  
682 extreme temperatures and humidities across various habitats in a large (200 x 300 km) and  
683 diverse region. *International Journal of Climatology*, **32**, 2134-2148.

684 Ashcroft, M.B. & Gollan, J.R. (2013) Moisture, thermal inertia, and the spatial distributions of near-  
685 surface soil and air temperatures: Understanding factors that promote microrefugia.  
686 *Agricultural and Forest Meteorology*, **176**, 77-89.

687 Ashcroft, M.B., Chisholm, L.A. & French, K.O. (2008) The effect of exposure on landscape scale soil  
688 surface temperatures and species distribution models. *Landscape Ecology*, **23**, 211-225.

689 Austin, M.P. & Van Niel, K.P. (2011) Improving species distribution models for climate change studies:  
690 variable selection and scale. *Journal of Biogeography*, **38**, 1-8.

691 Baddeley, A., Rubak, E. & Turner, R. (2015) *Spatial Point Patterns: Methodology and Applications with*  
692 *R*.

693 Bates, D., Maechler, M., Bolker, B. & Walker, S. (2013) lme4: linear mixed-effects models using Eigen  
694 and S4. In, R package version 1.0-5.

695 Bennie, J., Wilson, R.J., Maclean, I.M.D. & Suggitt, A.J. (2014) Seeing the woods for the trees - when is  
696 microclimate important in species distribution models? *Global Change Biology*, **20**, 2699-  
697 2700.

698 Bisrat, S.A., White, M.A., Beard, K.H. & Richard Cutler, D. (2012) Predicting the distribution potential  
699 of an invasive frog using remotely sensed data in Hawaii. *Diversity and Distributions*, **18**, 648-  
700 660.

701 Bond, W.J. & Midgley, J.J. (2001) Ecology of sprouting in woody plants: the persistence niche. *Trends*  
702 *in ecology & evolution*, **16**, 45-51.

703 Bramer, I., Anderson, B., Bennie, J., Bladon, A., De Frenne, P., Hemming, D., Hill, R.A., Kearney, M.R.,  
704 Körner, C., Korstjens, A.H., Lenoir, J., Maclean, I.M.D., Marsh, C.D., Morecroft, M.D.,  
705 Ohlemüller, R., Slater, H.D., Suggitt, A.J., Zellweger, F. & Gillingham, P.K. (2018) Advances in  
706 monitoring and modelling climate at ecologically relevant scales. *Advances in Ecological*  
707 *Research*,

708 Buermann, W., Saatchi, S., Smith, T.B., Zutta, B.R., Chaves, J.A., Milá, B. & Graham, C.H. (2008)  
709 Predicting species distributions across the Amazonian and Andean regions using remote  
710 sensing data. *Journal of Biogeography*, **35**, 1160-1176.

711 Cohen, J. (1994) Snow cover and climate. *Weather*, **49**, 150-156.

712 Cook, M.J. (2014) Atmospheric Compensation for a Landsat Land Surface Temperature Product.

713 Cord, A. & Rödder, D. (2011) Inclusion of habitat availability in species distribution models through  
714 multi-temporal remote-sensing data? *Ecological Applications*, **21**, 3285-3298.

715 De Frenne, P., Zellweger, F., Rodríguez-Sánchez, F., Scheffers, B.R., Hylander, K., Luoto, M., Vellend,  
716 M., Verheyen, K. & Lenoir, J. (2019) Global buffering of temperatures under forest canopies.  
717 *Nature Ecology & Evolution*, **1**.

718 Dee, D.P., Uppala, S., Simmons, A., Berrisford, P., Poli, P., Kobayashi, S., Andrae, U., Balmaseda, M.,  
719 Balsamo, G. & Bauer, d.P. (2011) The ERA-Interim reanalysis: Configuration and performance  
720 of the data assimilation system. *Quarterly Journal of the royal meteorological society*, **137**,  
721 553-597.

722 Distler, T., Schuetz, J.G., Velásquez-Tibatá, J. & Langham, G.M. (2015) Stacked species distribution  
723 models and macroecological models provide congruent projections of avian species richness  
724 under climate change. *Journal of Biogeography*, **42**, 976-988.

725 Dobrowski, S.Z. (2011) A climatic basis for microrefugia: the influence of terrain on climate. *Global*  
726 *Change Biology*, **17**, 1022-1035.

727 Dorrepaal, E., Aerts, R., Cornelissen, J.H., Callaghan, T.V. & Van Logtestijn, R.S. (2004) Summer  
728 warming and increased winter snow cover affect *Sphagnum fuscum* growth, structure and  
729 production in a sub-arctic bog. *Global Change Biology*, **10**, 93-104.

730 Elith, J. & Leathwick, J.R. (2009) Species Distribution Models: ecological explanation and prediction  
731 across space and time. *Annual Review of Ecology Evolution and Systematics*, pp. 677-697.

732 Fick, S.E. & Hijmans, R.J. (2017) WorldClim 2: new 1-km spatial resolution climate surfaces for global  
733 land areas. *International Journal of Climatology*, **37**, 4302-4315.

734 Fotheringham, A., Brunsdon, C. & Charlton, M. (2003) *Geographically weighted regression: the*  
735 *analysis of spatially varying relationships*. John Wiley & Sons, Hoboken, USA.

736 Fox, J. & Weisberg, S. (2011) *An {R} Companion to Applied Regression, Second Edition*.

737 Geiger, R. (1950) *The climate near the ground*. Harvard University Press, Cambridge, Massachusets,  
738 USA.

739 Gillingham, P.K., Huntley, B., Kunin, W.E. & Thomas, C.D. (2012) The effect of spatial resolution on  
740 projected responses to climate warming. *Diversity and Distributions*, **18**, 990-1000.

741 Gonzalez-Moreno, P., Diez, J.M., Richardson, D.M. & Vila, M. (2015) Beyond climate: disturbance  
742 niche shifts in invasive species. *Global Ecology and Biogeography*, **24**, 360-370.

743 Gottfried, M., Pauli, H., Reiter, K. & Grabherr, G. (1999) A fine-scaled predictive model for changes in  
744 species distribution patterns of high mountain plants induced by climate warming. *Diversity*  
745 *and Distributions*, **5**, 241-251.

746 Graae, B.J., De Frenne, P., Kolb, A., Brunet, J., Chabrerie, O., Verheyen, K., Pepin, N., Heinken, T.,  
747 Zobel, M., Shevtsova, A., Nijs, I. & Milbau, A. (2012) On the use of weather data in ecological  
748 studies along altitudinal and latitudinal gradients. *Oikos*, **121**, 3-19.

749 Graae, B.J., Vandvik, V., Armbruster, W.S., Eiserhardt, W.L., Svenning, J.-C., Hylander, K., Ehrlén, J.,  
750 Speed, J.D., Klanderud, K., Bråthen, K.A., Milbau, A., Opedal, O.H., Alsos, I.G., Ejrnaes, R.,  
751 Bruun, H.H., Birks, H.J.B., Westergaard, K.B., Birks, H.H. & Lenoir, J. (2018) Stay or go—how  
752 topographic complexity influences alpine plant population and community responses to  
753 climate change. *Perspectives in Plant Ecology, Evolution and Systematics*, **30**, 41-50.

754 Greiser, C., Meineri, E., Luoto, M., Ehrlén, J. & Hylander, K. (2018) Monthly microclimate models in a  
755 managed boreal forest landscape. *Agricultural and Forest Meteorology*, **250**, 147-158.

756 Guisan, A. & Thuiller, W. (2007) Predicting species distribution: offering more than simple habitat  
757 models (vol 8, pg 993, 2005). *Ecology Letters*, **10**, 435-435.

758 Hannah, L., Flint, L., Syphard, A.D., Moritz, M.A., Buckley, L.B. & McCullough, I.M. (2014) Fine-grain  
759 modeling of species' response to climate change: holdouts, stepping-stones, and  
760 microrefugia. *Trends in Ecology & Evolution*, **29**, 390-397.

761 Haylock, M., Hofstra, N., Klein Tank, A., Klok, E., Jones, P. & New, M. (2008) A European daily high-  
762 resolution gridded data set of surface temperature and precipitation for 1950–2006. *Journal*  
763 *of Geophysical Research: Atmospheres*, **113**

764 Hijmans, R.J., Cameron, S.E., Parra, J.L., Jones, P.G. & Jarvis, A. (2005) Very high resolution  
765 interpolated climate surfaces for global land areas. *International Journal of Climatology*, **25**,  
766 1965-1978.

767 Holden, Z.A., Abatzoglou, J.T., Luce, C.H. & Baggett, L.S. (2011) Empirical downscaling of daily  
768 minimum air temperature at very fine resolutions in complex terrain. *Agricultural and Forest*  
769 *Meteorology*, **151**, 1066-1073.

770 Illan, J.G., Gutierrez, D. & Wilson, R.J. (2010) The contributions of topoclimate and land cover to  
771 species distributions and abundance: fine-resolution tests for a mountain butterfly fauna.  
772 *Global Ecology and Biogeography*, **19**, 159-173.

773 Jiménez-Valverde, A., Peterson, A.T., Soberon, J., Overton, J.M., Aragon, P. & Lobo, J.M. (2011) Use of  
774 niche models in invasive species risk assessments. *Biological Invasions*, **13**, 2785-2797.

775 Jiménez-Valverde, A. (2012) Insights into the area under the receiver operating characteristic curve  
776 (AUC) as a discrimination measure in species distribution modelling. *Global Ecology and*  
777 *Biogeography*, **21**, 498-507.

778 Karger, D.N., Conrad, O., Böhner, J., Kawohl, T., Kreft, H., Soria-Auza, R.W., Zimmermann, N.E.,  
779 Linder, H.P. & Kessler, M. (2017) Climatologies at high resolution for the earth's land surface  
780 areas. *Scientific Data*, **4**, 170122.

781 Keppel, G., Mokany, K., Wardell-Johnson, G.W., Phillips, B.L., Welbergen, J.A. & Reside, A.E. (2015)  
782 The capacity of refugia for conservation planning under climate change. *Frontiers in Ecology  
783 and the Environment*, **13**, 106-112.

784 Körner, C. (2003) *Alpine plant life: functional plant ecology of high mountain ecosystems*. Springer,  
785 Berlin Heidelberg, Germany.

786 Körner, C. & Hiltbrunner, E. (2018) The 90 ways to describe plant temperature. *Perspectives in Plant  
787 Ecology, Evolution and Systematics*, **30**, 16-21.

788 Lembrechts, J., Nijs, I. & Lenoir, J. (2018) Incorporating microclimate into species distribution models.  
789 *Ecography*,

790 Lembrechts, J.J., Milbau, A. & Nijs, I. (2014) Alien roadside species more easily invade alpine than  
791 lowland plant communities in a subarctic mountain ecosystem. *PLoS One*, **9**, e89664.

792 Lembrechts, J.J., Lenoir, J., Nuñez, M.A., Pauchard, A., Geron, C., Bussé, G., Milbau, A. & Nijs, I. (2017)  
793 Microclimate variability in alpine ecosystems as stepping stones for non-native plant  
794 establishment above their current elevational limit. *Ecography*, **40**, 001-009.

795 Lembrechts, J.J., Pauchard, A., Lenoir, J., Nuñez, M.A., Geron, C., Ven, A., Bravo-Monasterio, P.,  
796 Teneb, E., Nijs, I. & Milbau, A. (2016) Disturbance is the key to plant invasions in cold  
797 environments. *Proceedings of the National Academy of Sciences of the United States of  
798 America*, **113**, 14061-14066.

799 Lenoir, J., Hattab, T. & Pierre, G. (2017) Climatic microrefugia under anthropogenic climate change:  
800 implications for species redistribution. *Ecography*, **40**, 253-266.

801 Lenoir, J., Graae, B.J., Aarrestad, P.A., Alsos, I.G., Armbruster, W.S., Austrheim, G., Bergendorff, C.,  
802 Birks, H.J.B., Brathen, K.A., Brunet, J., Bruun, H.H., Dahlberg, C.J., Decocq, G., Diekmann, M.,  
803 Dynesius, M., Ejrnaes, R., Grytnes, J.A., Hylander, K., Klanderud, K., Luoto, M., Milbau, A.,  
804 Moora, M., Nygaard, B., Odland, A., Ravolainen, V.T., Reinhardt, S., Sandvik, S.M., Schei, F.H.,  
805 Speed, J.D.M., Tveraabak, L.U., Vandvik, V., Velle, L.G., Virtanen, R., Zobel, M. & Svenning,  
806 J.C. (2013) Local temperatures inferred from plant communities suggest strong spatial  
807 buffering of climate warming across Northern Europe. *Global Change Biology*, **19**, 1470-1481.

808 Maclean, I.M.D., Suggitt, A.J., Wilson, R.J., Duffy, J.P. & Bennie, J.J. (2017) Fine-scale climate change:  
809 modelling spatial variation in biologically meaningful rates of warming. *Global Change  
810 Biology*, **23**, 256-268.

811 McCullough, I.M., Davis, F.W., Dingman, J.R., Flint, L.E., Flint, A.L., Serra-Diaz, J.M., Syphard, A.D.,  
812 Moritz, M.A., Hannah, L. & Franklin, J. (2016) High and dry: high elevations  
813 disproportionately exposed to regional climate change in Mediterranean-climate landscapes.  
814 *Landscape ecology*, **31**, 1063-1075.

815 Meineri, E. & Hylander, K. (2017) Fine-grain, large-domain climate models based on climate station  
816 and comprehensive topographic information improve microrefugia detection. *Ecography*, **40**,  
817 1003-1013.

818 Metz, M., Rocchini, D. & Neteler, M. (2014) Surface temperatures at the continental scale: tracking  
819 changes with remote sensing at unprecedented detail. *Remote Sensing*, **6**, 3822.

820 Nakagawa, S. & Schielzeth, H. (2013) A general and simple method for obtaining R<sup>2</sup> from generalized  
821 linear mixed-effects models. *Methods in Ecology and Evolution*, **4**, 133-142.

822 Neteler, M., Rocchini, D., Delucchi, L. & Metz, M. (2014) Massive data processing in GRASS GIS 7: A  
823 new gap-filled MODIS Land Surface Temperature time series data set. *FOSS4G-Europe 2014*  
824 (ed by).

825 Neteler, M., Metz, M., Rocchini, D., Rizzoli, A., Flacio, E., Engeler, L., Guidi, V., Lüthy, P. & Tonolla, M.  
826 (2013) Is Switzerland suitable for the invasion of *Aedes albopictus*? *PLoS One*, **8**, e82090.

827 Niittynen, P. & Luoto, M. (2017) The importance of snow in species distribution models of arctic  
828 vegetation. *Ecography*,

829 Opedal, O.H., Armbruster, W.S. & Graae, B.J. (2015) Linking small-scale topography with  
830 microclimate, plant species diversity and intra-specific trait variation in an alpine landscape.  
831 *Plant Ecology & Diversity*, **8**, 305-315.

832 Pauchard, A., Kueffer, C., Dietz, H., Daehler, C.C., Alexander, J., Edwards, P.J., Arévalo, J.R., Cavieres,  
833 L.A., Guisan, A., Haider, S., Jakobs, G., McDougall, K., Millar, C.I., Naylor, B.J., Parks, C.G., Rew,  
834 L.J. & Seipel, T. (2009) Ain't no mountain high enough: plant invasions reaching new  
835 elevations. *Frontiers in Ecology and the Environment*, **7**, 479-486.

836 Pauli, J.N., Zuckerberg, B., Whiteman, J.P. & Porter, W. (2013) The subnivium: a deteriorating  
837 seasonal refugium. *Frontiers in Ecology and the Environment*, **11**, 260-267.

838 Poorter, H., Fiorani, F., Pieruschka, R., Wojciechowski, T., van der Putten, W.H., Kleyer, M., Schurr, U.  
839 & Postma, J. (2016) Pampered inside, pestered outside? Differences and similarities between  
840 plants growing in controlled conditions and in the field. *New Phytologist*, **212**, 838-855.

841 Potter, K.A., Woods, H.A. & Pincebourde, S. (2013) Microclimatic challenges in global change biology.  
842 *Global Change Biology*, **19**, 2932-2939.

843 Pottier, J., Malenovský, Z., Psomas, A., Homolová, L., Schaepman, M.E., Choler, P., Thuiller, W.,  
844 Guisan, A. & Zimmermann, N.E. (2014) Modelling plant species distribution in alpine  
845 grasslands using airborne imaging spectroscopy. *Biology letters*, **10**, 20140347.

846 Pradervand, J.-N., Dubuis, A., Pellissier, L., Guisan, A. & Randin, C. (2014) Very high resolution  
847 environmental predictors in species distribution models: Moving beyond topography?  
848 *Progress in Physical Geography*, **38**, 79-96.

849 R Core Team (2015) *R: a language and environment for statistical computing*. R Foundation for  
850 Statistical Computing.

851 Randin, C.F., Vuissoz, G., Liston, G.E., Vittoz, P. & Guisan, A. (2009a) Introduction of snow and  
852 geomorphic disturbance variables into predictive models of alpine plant distribution in the  
853 Western Swiss Alps. *Arctic, Antarctic, and Alpine Research*, **41**, 347-361.

854 Randin, C.F., Engler, R., Normand, S., Zappa, M., Zimmermann, N.E., Pearman, P.B., Vittoz, P.,  
855 Thuiller, W. & Guisan, A. (2009b) Climate change and plant distribution: local models predict  
856 high-elevation persistence. *Global Change Biology*, **15**, 1557-1569.

857 Rebaudo, F., Faye, E. & Dangles, O. (2016) Microclimate data improve predictions of insect  
858 abundance models based on calibrated spatiotemporal temperatures. *Frontiers in*  
859 *Physiology*, **7**, 139.

860 Scherrer, D. & Körner, C. (2011) Topographically controlled thermal-habitat differentiation buffers  
861 alpine plant diversity against climate warming. *Journal of Biogeography*, **38**, 406-416.

862 Sears, M.W., Raskin, E. & Angilletta, M.J. (2011) The world is not flat: defining relevant thermal  
863 landscapes in the context of climate change. *Integrative and Comparative Biology*, **51**, 666-  
864 675.

865 Shanks, R.E. (1956) Altitudinal and microclimatic relationships of soil temperature under natural  
866 vegetation. *Ecology*, **37**, 1-7.

867 Sing, T., Sander, O., Beerenwinkel, N. & Lengauer, T. (2005) ROCr: visualizing classifier performance  
868 in R. *Bioinformatics*, **21**, 7781.

869 Slavich, E., Warton, D.I., Ashcroft, M.B., Gollan, J.R. & Ramp, D. (2014) Topoclimate versus  
870 macroclimate: how does climate mapping methodology affect species distribution models  
871 and climate change projections? *Diversity and Distributions*, **20**, 952-963.

872 Stewart, L., Simonsen, C.E., Svenning, J.C., Schmidt, N.M. & Pellissier, L. (2018) Forecasted  
873 homogenization of high Arctic vegetation communities under climate change. *Journal of*  
874 *biogeography*, **45**, 2576-2587.

875 Su, Y.F., Foody, G.M. & Cheng, K.S. (2012) Spatial non-stationarity in the relationships between land  
876 cover and surface temperature in an urban heat island and its impacts on thermally sensitive  
877 populations. *Landscape and Urban Planning*, **107**, 172-180.

878 Thompson, K.L., Zuckerberg, B., Porter, W.P. & Pauli, J.N. (2018) The phenology of the subnivium.  
879 *Environmental Research Letters*, **13**, 064037.



- 880 Wan, Z., Hook, S. & Hulley, G. (2015) MOD11C2 MODIS/Terra Land Surface Temperature/Emissivity  
881 8-Day L3 Global 0.05Deg CMG V006 [Data set]. In, NASA EOSDIS LP DAAC.
- 882 Wan, Z.M. (2008) New refinements and validation of the MODIS Land-Surface  
883 Temperature/Emissivity products. *Remote Sensing of Environment*, **112**, 59-74.
- 884 Warren, D.L., Glor, R.E. & Turelli, M. (2008) Environmental niche equivalency versus conservatism:  
885 quantitative approaches to niche evolution. *Evolution*, **62**, 2868-2883.
- 886 Wason, J.W., Bevilacqua, E. & Dovciak, M. (2017) Climates on the move: Implications of climate  
887 warming for species distributions in mountains of the northeastern United States.  
888 *Agricultural and Forest Meteorology*, **246**, 272-280.
- 889 Wild, J., Kopecký, M., Macek, M., Šanda, M., Jankovec, J. & Haase, T. (2019) Climate at ecologically  
890 relevant scales: A new temperature and soil moisture logger for long-term microclimate  
891 measurement. *Agricultural and Forest Meteorology*, **268**, 40-47.
- 892 Williams, C.M., Henry, H.A.L. & Sinclair, B.J. (2015) Cold truths: how winter drives responses of  
893 terrestrial organisms to climate change. *Biological Reviews*, **90**, 214-235.
- 894 Willis, K.J. & Bhagwat, S.A. (2009) Biodiversity and climate change. *Science*, **326**, 806-807.
- 895 Wood, S. (2006) *Generalized Additive Models: An introduction with R*. Chapman and Hall/CRC.
- 896 Wundram, D., Pape, R. & Löffler, J. (2010) Alpine soil temperature variability at multiple scales. *Arctic*  
897 *Antarctic and Alpine Research*, **42**, 117-128.
- 898 Yannic, G., Pellissier, L., Le Corre, M., Dussault, C., Bernatchez, L. & Côté, S.D. (2014) Temporally  
899 dynamic habitat suitability predicts genetic relatedness among caribou. *Proceedings of the*  
900 *Royal Society of London B: Biological Sciences*, **281**, 20140502.
- 901 Zellweger, F., De Frenne, P., Lenoir, J., Rocchini, D. & Coomes, D. (2019) Advances in microclimate  
902 ecology arising from remote sensing. *Trends in ecology & evolution*,
- 903 Zhang, T. (2005) Influence of the seasonal snow cover on the ground thermal regime: An overview.  
904 *Reviews of Geophysics*, **43**
- 905 Zuur, A.F., Ieno, E.N., Walker, N.J., Saveliev, A.A. & Smith, G.M. (2009) *Mixed effects models and*  
906 *extensions in ecology with R*. Springer, New York, USA.

907

## 908 **Data Accessibility Statement**

909 Most used climate datasets are freely available (see Methods section). In-situ soil temperature  
910 and species distribution data will be published in an open access data repository.

911 **Tables**

912 *Table 1: The eight studied climate datasets and their geographical and temporal extent, spatial resolution and measurement focus.*

<b>Dataset</b>	<b>Initial source</b>	<b>Geographical extent</b>	<b>Spatial resolution</b>	<b>Measurement focus</b>	<b>Temporal coverage</b>
a) WorldClim	WorldClim	Global	30''	Free-air	1970-2000
b) CHELSA	CHELSA	Global	30''	Free-air	1979-2013
c) Downscaled	CHELSA	10000 km <sup>2</sup>	1''	Free-air	1979-2013
d) Topoclimate	Aalto et al. (2018)	10000 km <sup>2</sup>	1''	Free-air	1981-2010
e) MODIS LST	MODIS	Global	30''	Surface	2015-2017
f) EuroLST	MODIS	Europe	~7.5''	Surface	2001-2011
g) E-OBS	E-OBS	Europe	0.1°	Free-air	2015-2017
h) Soil temperature	iButtons	10000 km <sup>2</sup>	1''	Soil	2015-2017

913

914 **Table 2: Overview of in-situ soil temperature measurement plots in Sweden and Norway (n=106).** For each gradient (numbers from 1) to 4)  
 915 refer to the map in Fig. 1), we present the number of elevation gradients (i.e. different mountains monitored), sites and plots (with more plots  
 916 than sites indicating repeated temperature measurements in a  $< 20 \times 20$  m area), as well as the temporal extent, the length of the elevation  
 917 gradient, and if species data is available to run species distribution models (SDMs).

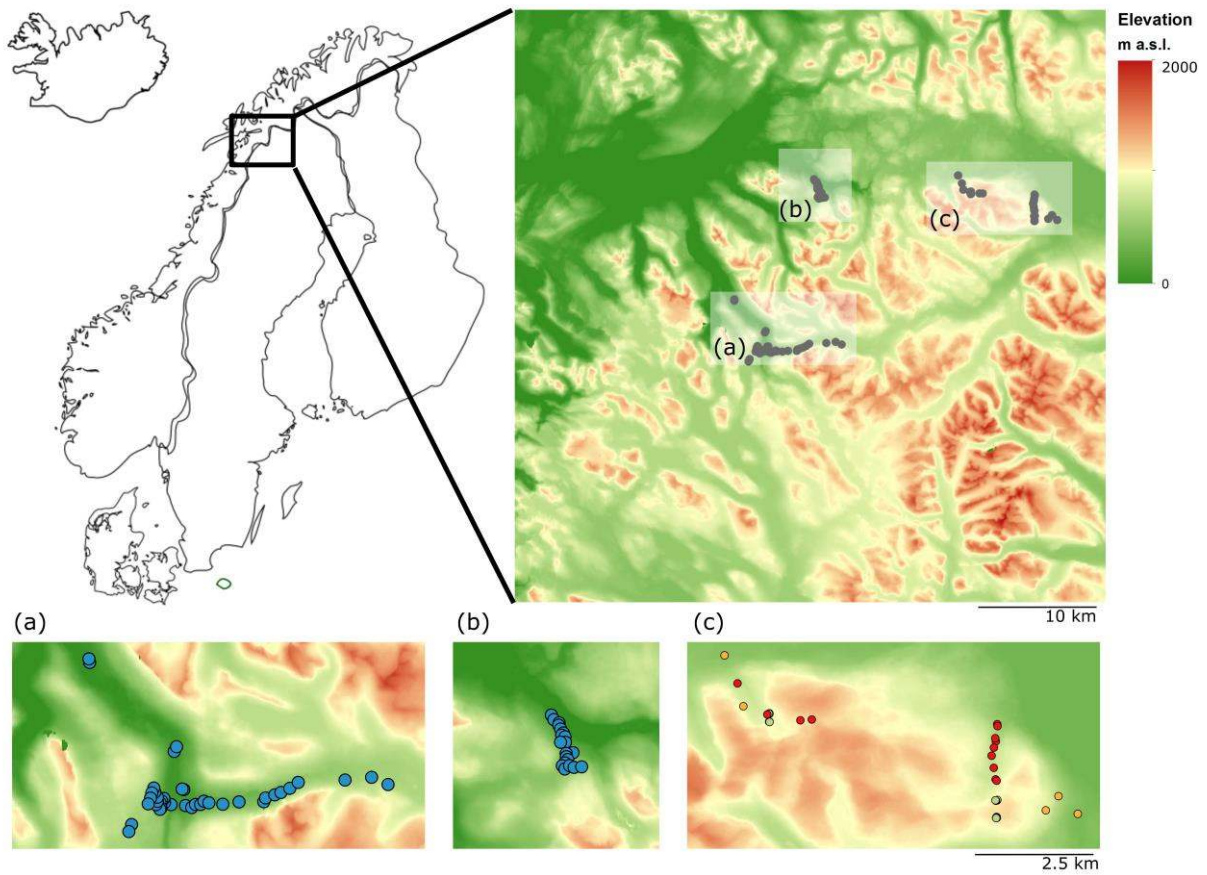
<b>Region</b>	<b>#</b>	<b>of Sites</b>	<b>Plots</b>	<b>Surface area</b>	<b>Temporal extent</b>	<b>Elevation (m a.s.l.)</b>	<b>Species data</b>
		<b>gradients</b>					
1) Norway	3	59	59	2 × 100 m	01/08/15-31/07/17	0-700	Yes
2) Sweden	2	4	23	0.6 × 1.2 m	01/08/15-31/07/16	900-1100	No
3) Sweden	2	6	11	0.6 × 1.2 m	01/08/16-31/07/17	400-900	No
4) Sweden	2	13	13	2 × 10 m	01/08/16-31/07/17	400-1200	No

918

919 **Table 3: Differences in average temperature between the climatic datasets.** Two-by-two  
920 comparisons between the three studied bioclimatic variables (*Bio1* = mean annual  
921 temperature, *Bio10* = mean temperature of the warmest quarter, *Bio11* = mean temperature  
922 of the coldest quarter) for the different climatic datasets (except WorldClim) after correcting  
923 for inter-annual and climate change effects using ERA Interim (see methods for details).  
924 Analysis based on data from all 106 measurement locations, for MODIS LST, E-OBS and in-  
925 situ soil temperature, only the data from 2016-2017 is tested. Values show the differences in  
926 average temperature in °C between the two datasets, with positive values indicating higher  
927 temperatures in the variable in the column than in the row. Values in bold are significant at  
928  $p < 0.05$  from paired *t*-tests. Relationships with in-situ soil temperature are visualised in Fig.  
929 S1, while some relationships among the other variables are visualised in Fig. S2.

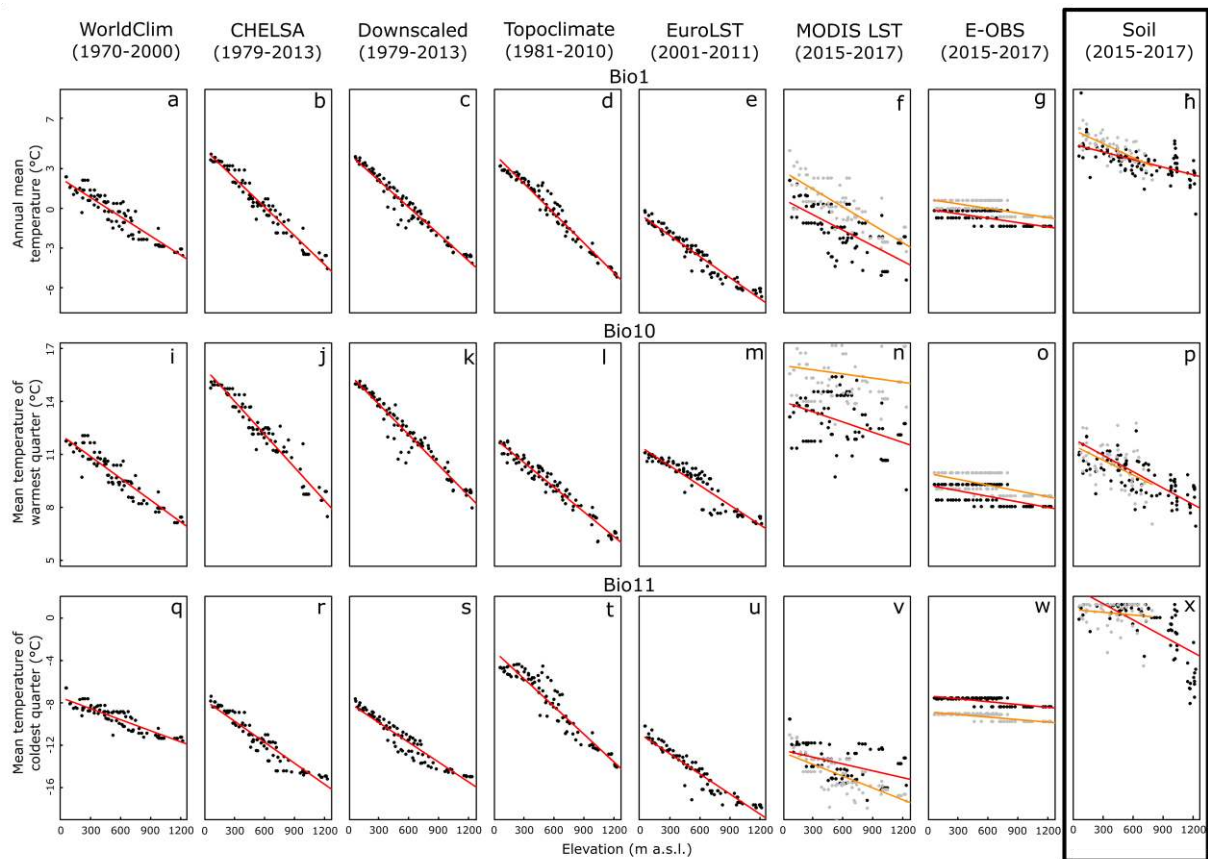
	CHELSA down	Topo- climate	EuroLST	MODIS LST	E-OBS	In-situ soil
<b>Bio1</b>						
CHELSA	-0.03	<b>-0.36</b>	<b>-3.19</b>	<b>-1.96</b>	<b>-1.11</b>	<b>2.67</b>
CHELSA down	-	<b>-0.33</b>	<b>-3.16</b>	<b>-1.92</b>	<b>-1.08</b>	<b>2.68</b>
Topoclimate	-	-	<b>-2.84</b>	<b>-1.59</b>	<b>-0.75</b>	<b>3.00</b>
EuroLST	-	-	-	<b>1.22</b>	<b>2.08</b>	<b>5.77</b>
MODIS LST	-	-	-	-	<b>0.91</b>	<b>4.53</b>
E-OBS	-	-	-	-	-	<b>3.53</b>
<b>Bio10</b>						
CHELSA	-0.03	<b>-2.86</b>	<b>-3.28</b>	<b>1.45</b>	<b>-2.85</b>	<b>-1.48</b>
CHELSA down	-	<b>-2.83</b>	<b>-3.25</b>	<b>1.49</b>	<b>-2.81</b>	<b>-1.48</b>
Topoclimate	-	-	<b>-0.42</b>	<b>4.30</b>	<b>0.01</b>	<b>1.24</b>
EuroLST	-	-	-	<b>4.70</b>	<b>0.43</b>	<b>1.67</b>
MODIS LST	-	-	-	-	<b>-4.23</b>	<b>-3.15</b>
E-OBS	-	-	-	-	-	<b>1.12</b>
<b>Bio11</b>						
CHELSA	-0.03	<b>2.60</b>	<b>-2.47</b>	<b>-4.82</b>	<b>0.02</b>	<b>6.30</b>
CHELSA down	-	<b>2.63</b>	<b>-2.44</b>	<b>-4.78</b>	<b>0.05</b>	<b>6.29</b>
Topoclimate	-	-	<b>-5.07</b>	<b>-7.39</b>	<b>-2.58</b>	<b>3.74</b>
EuroLST	-	-	-	<b>-2.35</b>	<b>2.49</b>	<b>8.72</b>
MODIS LST	-	-	-	-	<b>4.89</b>	<b>10.99</b>
E-OBS	-	-	-	-	-	<b>6.06</b>

930



932

933 **Figure 1: Study area and measurement locations.** Location of the study area in Scandinavia  
 934 (left) and digital elevation model (DEM) at 1 arc-second resolution (ca. 30 x 30 m at the  
 935 equator) across the study area (right). Dots on the DEM show locations of the 106 soil  
 936 temperature measurements. Species data sampling was done in the locations marked with  
 937 blue dots (a and b). See Table 2 for datasets: blue = 1), orange = 2), green = 3), red = 4).  
 938 Elevational gradients ranging from 0 till 700 m a.s.l. (a and b) and from 400 to 1200 m a.s.l.  
 939 (c).



940

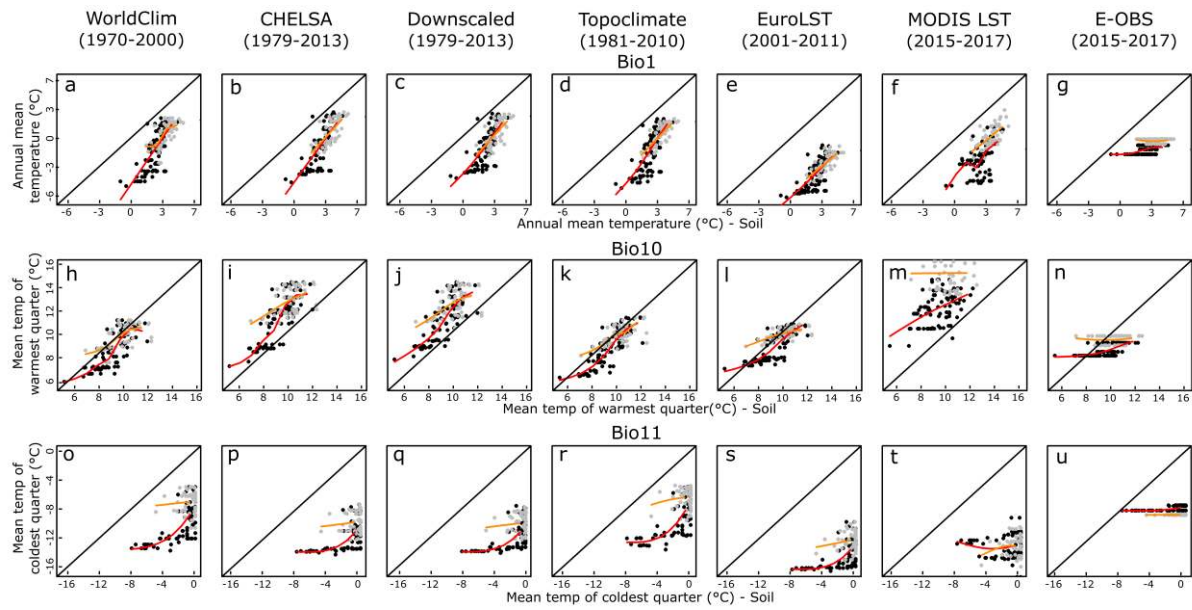
941 **Figure 2: Temperature patterns against elevation for the different temperature data sets.**

942 Average annual (Bio1, a-h), summer (Bio10, i-p) and winter (Bio11, q-x) temperature for the

943 eight climate datasets (columns, temporal extent between brackets) against elevation of the

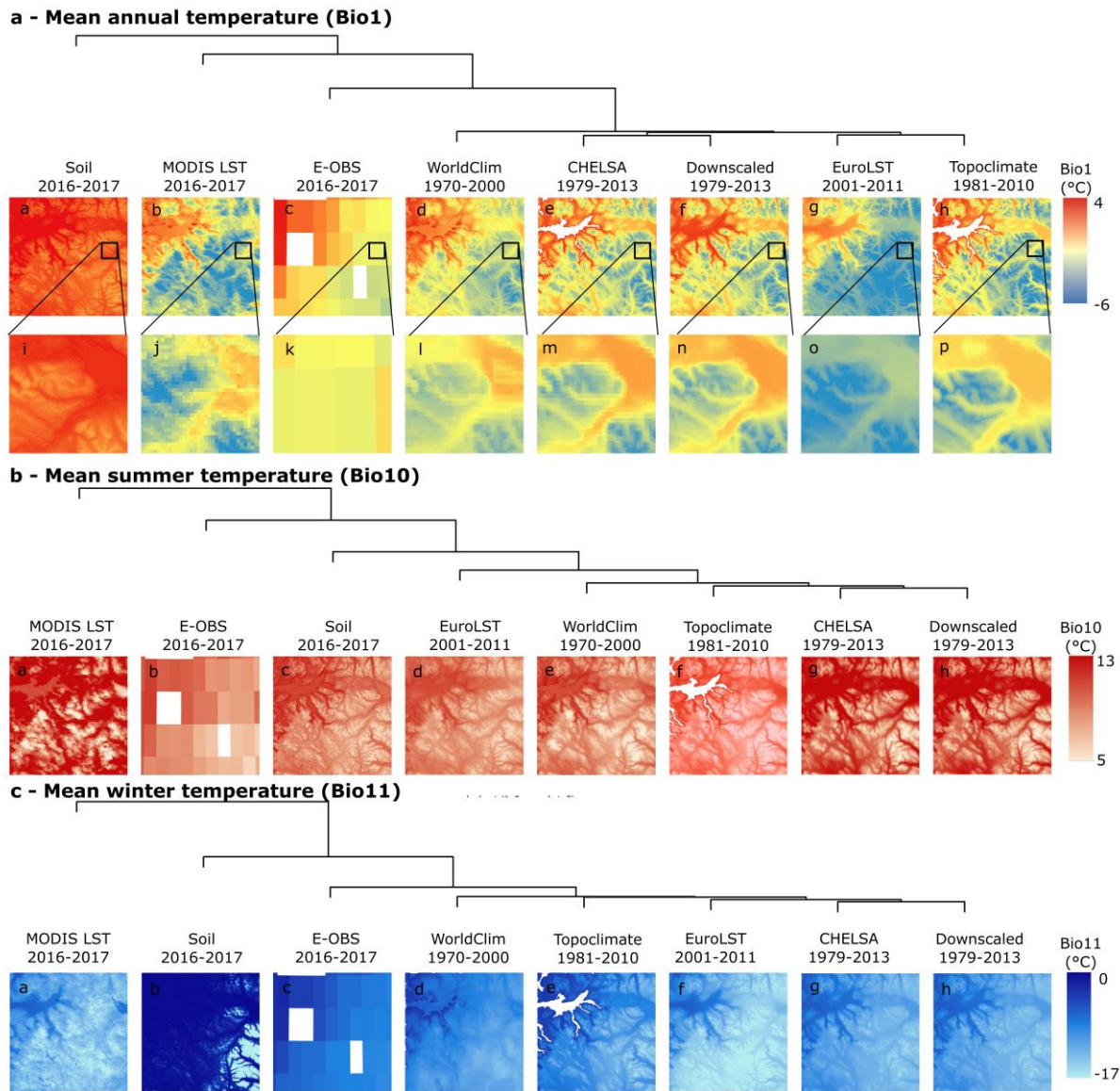
944 106 measurement locations. Orange (2015-2016) and red (2016-2017) lines are fitted with

945 linear models.



946

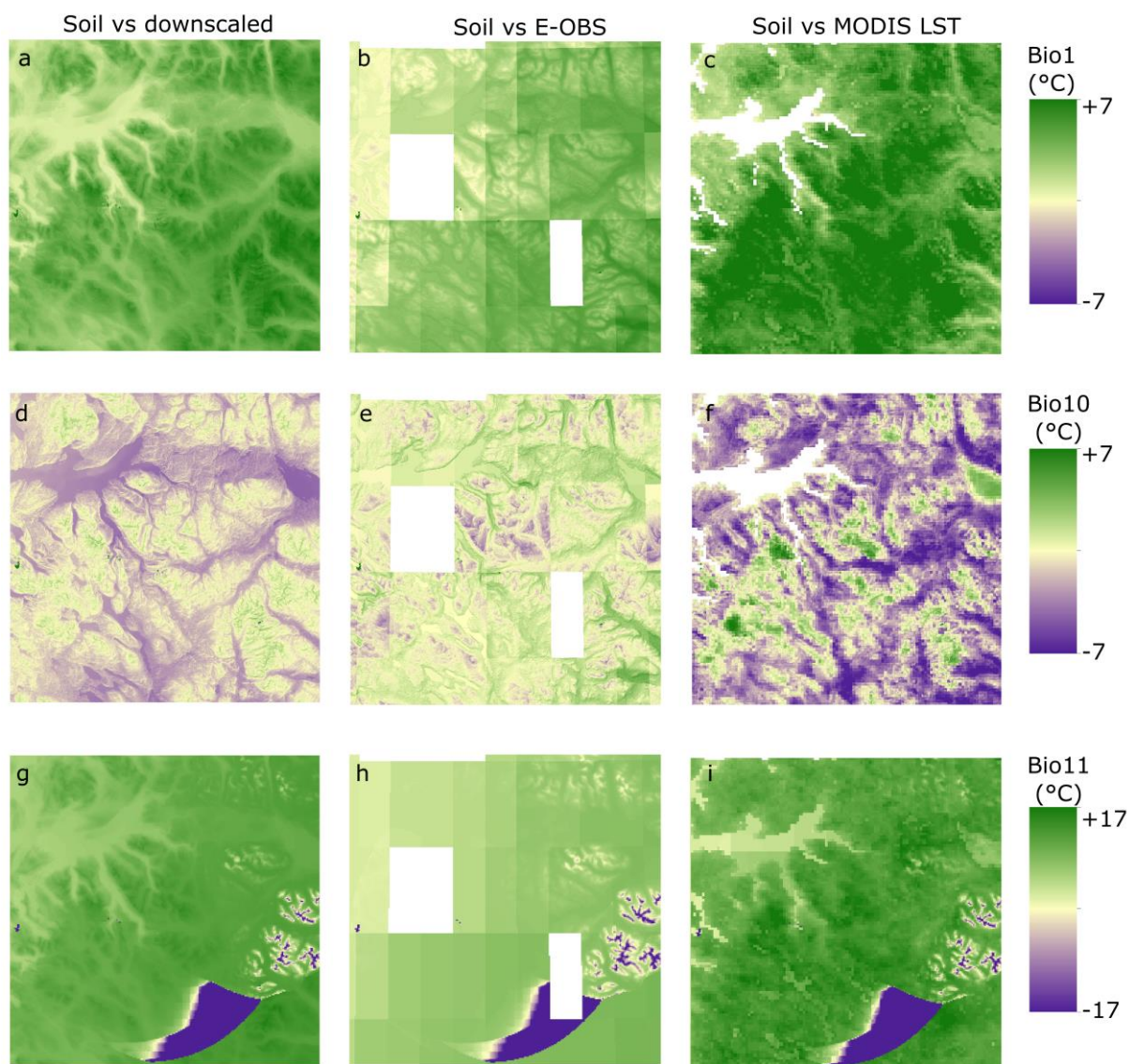
947 **Figure 3: Plot-by-plot comparisons of soil temperature data against 7 other sources of**  
 948 **temperature data. Mean annual (Bio1, a-g), summer (Bio10, h-n) and winter (Bio11, o-u)**  
 949 **temperature, for all 106 measurement locations for 2015-2016 (orange lines, grey dots) and**  
 950 **2016-2017 (red lines, black dots). Black lines show first bisectors (a hypothetical perfect**  
 951 **match), red and orange lines are fitted with generalised additive models for each year of**  
 952 **temperature measurements separately. Measurement periods between brackets.**



953

954 **Figure 4: Dendrograms of collinearity between different temperature datasets.** Data from  
 955 the 106 measurement locations for mean annual (a - Bio1), summer (b – Bio10) and winter (c  
 956 – Bio11) temperature. Measurement periods between brackets. Maps show the regional (100  
 957 × 100 km) predictions for each dataset and bioclimatic variable. For Bio1, cut-outs of the  
 958 maps are shown (location specified by black squares).

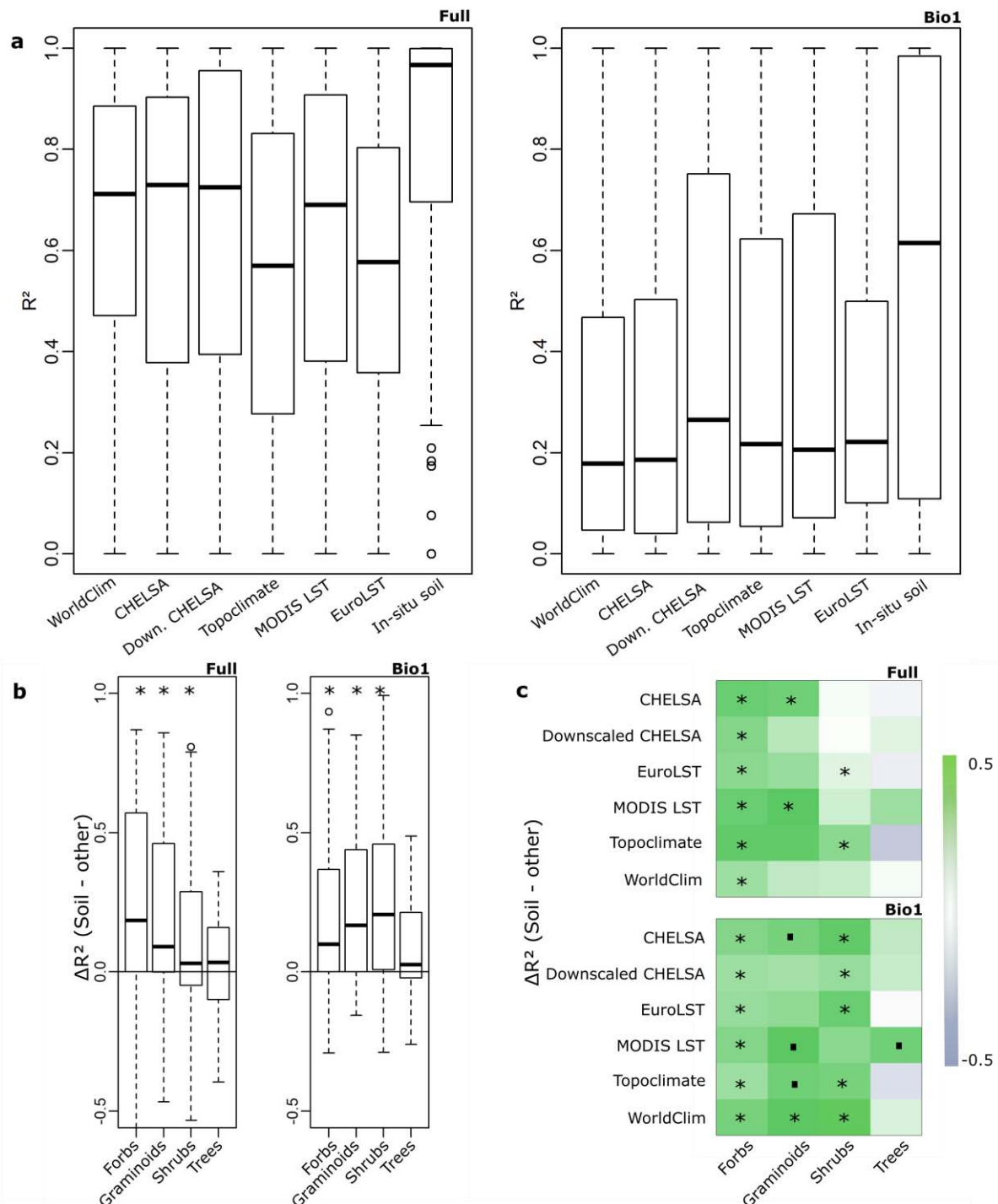




959

960 **Figure 5: Differences (in °C) between regionally modelled soil temperature and other**  
 961 **temperature data sources.** Differences in annual average temperature (Bio1), mean  
 962 temperature of the warmest quarter (Bio10) and mean temperature of the coldest quarter  
 963 (Bio11) are shown for soil temperature versus downscaled CHELSA (left), E-OBS (middle)  
 964 and MODIS LST (right). Comparisons between soil temperature and CHELSA, WorldClim  
 965 and EuroLST are not shown, as trends were similar. Values below zero indicate a lower value  
 966 for the soil temperature compared with the other dataset; values above zero a higher value.

967



968

969 **Figure 6: Proportion of explained variance (marginal  $R^2$ ) by species distribution models**

970 **(SDMs) using the different temperature datasets. (a) Boxplots of the marginal  $R^2$  of**

971 **distribution models for 50 plant species in a subset of 59 plots, based on binomial GLMMs**

972 **built with the different temperature datasets: using Bio1, 10 and 11 together (left, 'Full') or**

973 **Bio1 only (right, 'Bio1'). (b) Differences in marginal  $R^2$  between the models using soil**

974 *temperature and all other datasets for forbs (N = 25), graminoids (N = 7), (dwarf) shrubs (N*  
975 *= 15) and trees (N = 3). (c) Heatmaps visualising the differences in marginal R<sup>2</sup> between the*  
976 *models using soil temperature and each of the other climatic datasets for the different growth*  
977 *forms. Green (positive values) indicates better performance of soil temperature models, blue*  
978 *a better performance of the other dataset in question. “\*” and “.” respectively indicate*  
979 *significant ( $p < 0.05$ ) and marginally significant ( $0.05 < p < 0.1$ ) differences from zero as*  
980 *obtained with a two-sided t-test.*

981

982

983